

# Current Advances in the Methodology and Computational Simulation of the Formation of Low-Mass Stars

**Richard I. Klein**

University of California, Berkeley  
and Lawrence Livermore National Laboratory

**Shu-ichiro Inutsuka**

Kyoto University

**Paolo Padoan**

University of California, San Diego

**Kohji Tomisaka**

National Astronomical Observatory, Japan

Developing a theory of low-mass star formation ( $\sim 0.1$  to  $3 M_{\odot}$ ) remains one of the most elusive and important goals of theoretical astrophysics. The star-formation process is the outcome of the complex dynamics of interstellar gas involving non-linear interactions of turbulence, gravity, magnetic field and radiation. The evolution of protostellar condensations, from the moment they are assembled by turbulent flows to the time they reach stellar densities, spans an enormous range of scales, resulting in a major computational challenge for simulations. Since the previous Protostars and Planets conference, dramatic advances in the development of new numerical algorithmic techniques have been successfully implemented on large scale parallel supercomputers. Among such techniques, Adaptive Mesh Refinement and Smooth Particle Hydrodynamics have provided frameworks to simulate the process of low-mass star formation with a very large dynamic range. It is now feasible to explore the turbulent fragmentation of molecular clouds and the gravitational collapse of cores into stars self-consistently within the same calculation. The increased sophistication of these powerful methods comes with substantial caveats associated with the use of the techniques and the interpretation of the numerical results. In this review, we examine what has been accomplished in the field and present a critique of both numerical methods and scientific results. We stress that computational simulations should obey the available observational constraints and demonstrate numerical convergence. Failing this, results of numerical simulations do not advance our understanding of low-mass star formation.

## 1. INTRODUCTION

Most of the stars in the galaxy exist in gravitationally bound binary and low-order multiple systems. Although several mechanisms have been put forth to account for binary star formation, fragmentation has emerged as the leading mechanism in the past decade (Bodenheimer *et al.*, 2000). This point of view has been strengthened by observations that have shown the binary frequency among pre-main-sequence stars is comparable to or greater than that among nearby main-sequence stars (Duchene *et al.*, 1999). This suggests that most binary stars are formed during the protostellar collapse phase. Developing a theory for low mass star formation (0.1 to 3 solar masses), which explains the physical properties of the formation of binary and multiple stellar systems, remains one of the most elusive and important goals of theoretical astrophysics.

Until very recently, the extreme variations in length scale

inherent in the star formation process have made it difficult to perform accurate calculations of fragmentation and collapse, which are intrinsically three-dimensional in nature. Since the last review in *Protostars and Planets IV* by Bodenheimer *et al.*, 2000, dramatic advances in the development of new numerical algorithmic techniques, including adaptive mesh refinement (AMR) and Smooth Particle Hydrodynamics (SPH), as well as advances in large scale parallel machines, have allowed a significant increase in the dynamic range of simulations of low mass-star formation. It is now feasible to explore the turbulent fragmentation of molecular clouds and the gravitational collapse of cores into stars self-consistently within the same calculation. In this chapter we examine what has been recently accomplished in the field of numerical simulation of low-mass star formation, and we critically review both numerical methods and scientific results.

## 1.1. Key Questions Posed by the Observations

Observational surveys present us with a basic picture of star-forming regions including the structure and dynamics of star-forming clouds and the properties of protostellar cores. A theory of star-formation should explain both the large scale environment and the properties of protostellar cores self-consistently.

As shown first by *Larson* (1981), and later confirmed by many other studies, star-forming regions are characterized by a correlation between internal velocity dispersion and size,  $\delta V \approx 1\text{km/s}(L/1\text{pc})^{0.4}$ . This scaling law has been interpreted as evidence of supersonic turbulence on a wide range of scales. The turbulence can provide support against the gravitational collapse, but can also create gravitationally unstable compressed regions through shocks. A theory of star formation should elucidate whether turbulence controls the star formation rate and efficiency, or are those properties controlled by stellar outflows and winds? Are the scaling laws of turbulent flows related to scaling laws of core and stellar properties? Is the turbulence setting the initial density perturbations that collapse into stars? What is the effect of turbulence on the accretion of mass onto protostars?

On smaller scales, observational surveys have shown that prestellar cores are elongated. Their density profiles are flat near the center, steeper at larger radii, may show very sharp edges and are sometimes consistent with Bonnor-Ebert profiles (e.g., *Bacmann et al.*, 2000; *Alves et al.*, 2001). Cores have rotational energies on the average only a few percent of their binding energies (e.g., *Goodman et al.*, 1993). They are marginally supercritical (*Crutcher*, 1999) and their mass distribution is very similar to the stellar mass distribution (e.g., *Motte et al.*, 1998, 2001). The large majority of cores are found to contain stars (e.g., *Jijina et al.*, 1999), and individual cores produce at most 2-3 protostars (e.g., *Goodwin and Kroupa*, 2005). A theory of low-mass star formation should be consistent with these observations and address: Why are prestellar cores so short-lived? Why do they have Bonnor-Ebert profiles? How does the observed core angular momentum affect the formation of binary and multiple systems? What is the role played by magnetic fields in their evolution? Why is the mass distribution of prestellar cores so similar to the stellar initial mass function? Why are cores barely fragmenting into binaries or low multiplicity systems?

Observations of young stellar populations provide important constraints as well. We know that young stars are always found in association with dense gas with an efficiency  $\sim 10\text{-}20\%$ , much higher than the overall star formation efficiency in GMCs,  $\sim 1\text{-}3\%$  (e.g., *Myers et al.*, 1986). Stars are often found in clusters, of size ranging from 10 to 1000 members (e.g., *Lada and Lada*, 2003). The stellar initial mass function peaks around a fraction of a solar mass and its lognormal shape around the peak is roughly the same in open clusters, globular clusters and field stars (*Chabrier*, 2003). What determines the efficiency of star formation? Why is the stellar multiplicity higher in younger

populations? What determines the typical stellar mass and the initial mass function?

Although answering all these questions is outside the scope of this review, we pose them because these are the questions to be addressed by the computational simulations of the formation of low-mass stars.

## 1.2. Generation of Initial Conditions Consistent with the Observations

Simulations of low mass star formation should generate initial conditions for the collapse of protostars consistent with the observed physical properties of star forming clouds. This can be achieved if a relatively large scale is simulated ( $> 1\text{ pc}$ ) with numerical methods that can accurately reproduce fundamental statistics measured in molecular clouds. Such statistics include i) scaling laws of velocity, density and magnetic fields; ii) mean relative values of turbulent, thermal, magnetic and gravitational energies (the normalization of the scaling laws).

**1.2.1. Scaling Laws.** *Larson* (1981) found that velocity and size of interstellar clouds are correlated over many orders of magnitude in size. This correlation has been confirmed by many more recent studies (e.g., *Fuller and Myers*, 1992; *Falgarone et al.*, 1992). The most accepted interpretation is that the scaling law reflects the presence of supersonic turbulence in the ISM (e.g., *Larson*, 1981; *Ossenkopf and Mac-Low*, 2002; *Heyer and Brunt*, 2004). Large scale velocity-column density correlations from molecular line surveys of giant molecular clouds also suggest a turbulent origin of the observed density enhancements (*Padoan et al.*, 2001). Starting with the work of *Troland and Heiles* (1986), a correlation between magnetic field strength and gas density,  $B \propto n^{1/2}$ , has been reported for mean densities larger than  $n \sim 100\text{ cm}^{-3}$ . However, density and magnetic field scalings are very uncertain because both quantities are difficult to measure.

**1.2.2. Mean Energies.** Assuming an average temperature of  $T = 10\text{ K}$ , Larson's velocity-size correlation corresponds to an rms sonic Mach number  $M_s \approx 5$  on the scale of 1 pc, and  $M_s \approx 1$  at 0.02 pc. So, on the average, the turbulent kinetic energy is larger than the thermal energy. Indirect evidence of super-Alfvénic dynamics in giant molecular clouds has been presented by *Padoan and Nordlund* (1999) and *Padoan et al.* (2004a). They have shown that the magnetic energy averaged over a large scale has an intermediate value between the thermal and the kinetic energies, even if it can be significantly larger than this average value within dense prestellar cores. Observations suggest that in dense cores gravitational, kinetic, thermal and magnetic energies are all comparable. However, the magnetic energy is very difficult to estimate. Accounting for both detections and upper limits, there is a large dispersion in the ratio of magnetic to gravitational energy of dense cores (*Crutcher et al.*, 1993; *Crutcher et al.*, 1999; *Bourke et al.*, 2001; *Nutter et al.*, 2004). In the case of turbulence that is super-Alfvénic on the large scale, this dispersion and the

$B$ - $n$  relation are predicted to be real (*Padoan and Nordlund*, 1999).

In summary, large scale simulations may provide realistic initial and boundary conditions for protostellar collapse, but they must be consistent with the turbulent nature of the ISM. On the scale of giant molecular clouds, observations suggest the turbulence is on the average supersonic and super-Alfvénic and its kinetic energy is roughly equal to the cloud gravitational energy.

## 2. A BRIEF SURVEY OF LOW-MASS STAR FORMATION MECHANISMS

Although much progress in numerical simulations of collapse and fragmentation has been made in the intervening 6 years since PPIV, a self-consistent theory of binary and multiple star formation that addresses the key questions posed by observations is still not at hand. As discussed by *Bodenheimer et al.*, 2000, binary and multiple formation can occur through the processes of (i) capture, (ii) fission, (iii) prompt initial fragmentation, (iv) disk fragmentation and (v) fragmentation during the protostellar collapse phase.

A recent mechanism for multiple star formation has been put forth by *Shu et al.*, (2000) and *Galli et al.*, (2001). They develop equilibrium models of strongly magnetized isopadic disks and explored their bifurcation to non-axisymmetric, multi-lobed structures of increasing rotation rates. Possible problems with this mechanism include the observed low rotational energies, the observed random alignment of disks with the ambient magnetic fields, the complexity of star-forming regions relative to the two dimensional geometry and absence of turbulence in the model.

Disk fragmentation from gravitational instability can result in multiple systems in an equilibrium disk if the minimum Toomre  $Q$  parameter falls below  $\approx 1$ . However, *Bodenheimer et al.*, 2000, have pointed out that the required initial conditions to obtain  $Q < 1$  may not be easily realized since the mass accretion timescale is significantly longer than the dynamical timescale throughout most of the evolution of the protostar. Disk fragmentation plays a key role in one of the theories of the formation of Brown Dwarfs (BDs). This scenario, known as the "failed embryo" scenario, begins with a gravitationally unstable disk surrounding a protostar. The disk fragments into a number of sub-stellar objects. If the crossing time of the cluster of embryos is much less than the free-fall time of the collapsing core, one or more of the members will be rapidly ejected resulting in a BD (*Reipurth and Clarke*, 2001). Problems with this model include observational evidence of BD clustering (*Duchêne et al.*, 2004), Ly- $\alpha$  signatures of BD accretion (e.g., *Jayawardhana et al.*, 2002; *Natta et al.*, 2004; *Barrado y Navascués et al.*, 2004; *Mohanty et al.*, 2005) and evidence that individual cores produce only 2 or 3 stars (*Goodwin and Kroupa*, 2005).

Currently, there are two dominant models to explain

what determines the mass of stars. The Direct Gravitational Collapse theory suggests that star-forming turbulent clouds fragment into cores that eventually collapse to make individual stars or small multiple systems (*Shu et al.*, 1987; *Padoan and Nordlund*, 2002, 2004). In contrast, the Competitive Accretion theory suggests that at birth all stars are much smaller than the typical stellar mass and that the final stellar mass is determined by the subsequent accretion of unbound gas from the clump (*Bonnell et al.*, 1998; *Bonnell et al.*, 2001; *Bate et al.*, 2005). Significant problems with competitive accretion include the large value of the observed virial parameter relative to the one required by competitive accretion (*Krumholz et al.*, 2005b). We discuss this problem with competitive accretion in detail in section 4d.

## 3. PHYSICAL PROCESSES NECESSARY FOR DETAILED SIMULATION OF LOW-MASS STAR FORMATION

### 3.1. Turbulence

The Reynolds number estimates the relative importance of the nonlinear advection term and the viscosity term in the Navier-Stokes equation,  $Re = V_0 L_0 / \nu$ .  $V_0$  is the flow rms velocity,  $L_0$  is the integral scale of the turbulence (say the energy injection scale) and  $\nu$  is the kinematic viscosity that we can approximate as  $\nu \approx v_{th} / (\sigma n)$ .  $v_{th}$  is the gas thermal velocity,  $n$  is the gas mean number density and  $\sigma \sim 10^{-15} \text{ cm}^2$  is the typical gas collisional cross section. For typical molecular cloud values,  $Re \sim 10^7$ - $10^8$ , which implies flows are highly unstable to turbulence. It is important to recognize the significance of turbulent gas dynamics in astrophysical processes, as turbulence is a dominant transport mechanism. In molecular clouds, the turbulence is supersonic and the postshock gas cooling time is very short. This results in the highly fragmented structure of molecular clouds.

There has been significant progress in our understanding of supersonic turbulence in recent years (progress on the scaling properties of subsonic and sub-Alfvénic turbulence is reviewed in *Cho et al.*, 2003). Phenomenological models of the intermittency of incompressible turbulence (e.g., *She and Leveque*, 1994; *Dubrulle*, 1994) have been extended to supersonic turbulence by *Boldyrev* (2002) and the predictions of the model have been confirmed by numerical simulations (*Boldyrev et al.*, 2002a; *Padoan et al.*, 2004b). The intermittency correction is small for the exponent of the velocity power spectrum (corresponding to the second order velocity structure function) and large only at high order. However, *Boldyrev et al.* (2002b) have shown that low order density correlators depend on high order velocity statistics, so intermittency is likely to play a significant role in turbulent fragmentation, despite being only a small effect in the velocity power spectrum.

Because supersonic turbulence can naturally generate, at very small scale, strong density enhancements of mass comparable to a low mass stars or even a brown dwarf,

its correct description is of paramount importance for simulations of molecular cloud fragmentation into low mass stars and brown dwarfs. At present, the largest simulations of supersonic turbulence may achieve a Reynolds number  $Re \sim 10^4$ . The scale of turbulence dissipation is therefore much larger in numerical simulations (of order the computational mesh size) than in nature ( $\sim 10^{14}$  cm). However, the ratio of the Kolmogorov dissipation scale,  $\eta_K$ , and the Jeans length,  $\lambda_J$ , is very small and remarkably independent of temperature and density,  $\eta_K/\lambda_J \approx 10^{-4}(T/10\text{K})^{-1/8}(n/10^3\text{cm}^{-3})^{-1/4}$ . One may hope to successfully simulate the process of turbulent fragmentation by numerically resolving the turbulence to scales smaller than  $\lambda_J$ , but not as small as  $\eta_K$ , unless the nature of turbulent flows varies dramatically between  $Re \sim 10^3$  and  $Re \sim 10^7$ . Experimental results seem to indicate that the asymptotic behavior of turbulence is recovered in the approximate range  $Re = 10,000\text{--}20,000$  (Dimotakis, 2000), which can be achieved with PPM simulations on a  $2,048^3$  mesh.

In order to i) generate a sizable inertial range (a power law power spectrum of the turbulent velocity over an extended range of scales) and ii) resolve the turbulence just below the Jeans length, a minimum computational box size of at least  $1,000^3$  zones is required for a grid code. This accounts for the fact that the velocity power spectrum starts to decay with increasing wavenumber faster than a power law already at approximately 30 times the Nyquist frequency. It is still an optimistic estimate, because at this resolution the velocity power spectrum is also affected by the bottleneck effect (e.g., Falkovich, 1994; Dobler *et al.*, 2003; Haugen and Brandenburg, 2004). Assuming the standard SPH kernel of 50 particles, this corresponds to at least  $50 \times 1,000^3$  particles to describe the density field, and at least  $\text{few} \times 1,000^3$  particles to describe the velocity field, if a Godunov SPH method is used (see below).

Grid code simulations have started to achieve this dynamical range only recently, while particle codes appear unsuitable to the task. The calculation of Bate *et al.* (2003) has  $3.5 \times 100^3$  particles, more than four orders of magnitude below the above estimate and therefore inadequate to describe the process of turbulent fragmentation (the formation of small scale density enhancements by the supersonic turbulence). Studies proposing to directly test the effect of turbulence on star formation, based on numerical simulations with resolution well below the above estimate, should be regarded with caution.

## 3.2. Gravity

**3.2.1. The Jeans Condition.** Jeans (1902) analyzed the linearized equations of 1D isothermal self-gravitational hydrodynamics (GHD) for a medium of infinite extent and found that perturbations on scales larger than the Jeans length,  $\lambda_J \equiv (\frac{\pi c_s^2}{G\rho})^{1/2}$ , are unstable. Thermal pressure cannot resist the self-gravity of a perturbation larger than  $\lambda_J$ , resulting in runaway collapse. Truelove *et al.* (1997) showed

that the errors generated by numerical GHD solvers can act as unstable perturbations to the flow. In a simulation with variable resolution, cell-scale errors introduced in regions of coarser resolution can be advected to regions of finer resolution, allowing these errors to grow. The unstable collapse of numerical perturbations can lead to artificial fragmentation. The strategy to avoid artificial fragmentation is to maintain a sufficient resolution of  $\lambda_J$ . Defining the Jeans number  $J \equiv \frac{\Delta x}{\lambda_J}$ , Truelove *et al.* (1997) found that keeping  $J \leq 0.25$  avoided artificial fragmentation in the isothermal evolution of a collapse spanning 7 decades of density, the approximate range separating typical molecular cloud cores from nonisothermal protostellar fragments. This Jeans condition arises because perturbations on scales above  $\lambda_J$  are physically unstable, and discretization of the GHD PDEs introduces perturbations on all scales above  $\Delta x$ . It is essential to keep  $\lambda_J$  as resolved as possible in order to diminish the initial amplitude of perturbations that exceed this scale. Although it has been shown to hold only for isothermal evolution, it is reasonable to expect that it is necessary (although not necessarily sufficient) for nonisothermal collapse as well where the transition to non-isothermal evolution may produce structure on smaller scales than the local Jeans length. .

**3.2.2. Runaway Collapse.** The self-gravitational collapse in nearly spherical geometry tends to show a so-called “runaway collapse,” where the denser central region collapses much faster than the less-dense surrounding region. The mass of the central fast collapsing region is of the order of the Jeans mass,  $M_J = \rho\lambda_J^3 \sim G^{-3/2}C_s^{3/2}\rho^{-1/2}$ , which decreases monotonically in this runaway stage. The description of this process requires increasingly higher resolution, not only on the spatial scale but also on the mass scale. Therefore, an accurate description is not guaranteed even with Lagrangian particle methods such as SPH, if the number of particles is conserved. The end of the runaway stage corresponds to the deceleration of the gravitational collapse. If the effective ratio of specific heats,  $\gamma$  ( $P \propto \rho^\gamma$ ), becomes larger than  $\gamma_{\text{crit}} = 4/3$ , the increased pressure can decelerate the gravitational collapse. For example, the question of how and when the isothermal evolution terminates was explored in Masunaga and Inutsuka (1999).

**3.2.3. Thermal Budget.** In the low density regime the gas temperature is affected by various heating and cooling processes (e.g., Wolfire *et al.*, 1995; Koyama and Inutsuka, 2000; Juvela *et al.*, 2001). However, above a gas density of  $10^4\text{--}10^5\text{ cm}^{-3}$ , depending on the timescale of interest, the gas is thermally well coupled with the dust grains that maintain a temperature of order 10K. During the dynamical collapse, gas and dust are isothermal until a density of  $10^{10}\text{--}10^{11}\text{ cm}^{-3}$ , when the compressional heating rate becomes larger than the cooling rate (Inutsuka and Miyama, 1997; Masunaga and Inutsuka, 1999). The further evolution of a collapsing core and the formation of a protostar are radiation-hydrodynamical (RHD) processes that should be modeled by solving the radiation transfer and the hydrody-

namics simultaneously and in three dimensions. Presently, the most sophisticated multi-dimensional models are based on the (flux-limited) diffusion approximation (Bodenheimer *et al.* 1990, Krumholz *et al.* 2005c).

Once the compressional heating dominates the radiative cooling, the central temperature increases gradually from the initial value of  $\sim 10$  K. The initial slope of the temperature as a function of gas density corresponds to an effective ratio of specific heats  $\gamma = 5/3$ :  $T(\rho) \propto \rho^{2/3}$  for  $10\text{K} < T < 100\text{K}$ . This monatomic gas property is due to the fact that the rotational degree of freedom of molecular hydrogen is not excited in this low temperature regime (e.g.,  $E(J = 2 - 0)/k_B = 512\text{K}$ ). When the temperature becomes larger than  $\sim 10^2\text{K}$ , the slope corresponds to  $\gamma = 7/5$ , as for diatomic molecules. This value of  $\gamma$  is larger than the minimum required for thermal pressure support against gravitational collapse:  $\gamma > \gamma_{\text{crit}} \equiv 4/3$ . The collapse is therefore decelerated and a shock is formed at the surface of a quasi-adiabatic core, called “the first core”. Its radius is about 1 AU in spherically symmetric models, but can be significantly larger in more realistic multi-dimensional models. It consists mainly of H<sub>2</sub>.

The increase of density and temperature inside the first core is slow but monotonic. When the temperature becomes  $> 10^3$  K, the dissociation of H<sub>2</sub> starts. The dissociation of H<sub>2</sub> acts as an efficient cooling of the gas, which makes  $\gamma < 4/3$ , triggering the second dynamical collapse. In this second collapse phase, the collapsing velocity becomes very large and engulfs the first core. As a result, the first core lasts for only  $\sim 10^3$  years. In the course of the second collapse, the central density attains the stellar value,  $\rho \sim 1 \text{ g/cm}^3$ , and the second adiabatic core, or “protostar”, is formed. The time evolution of the SED obtained from the self-consistent RHD calculation can be found in Masunaga *et al.* (1998) and Masunaga and Inutsuka (2000a,b).

**3.2.4. Core Fragmentation.** Tsuribe and Inutsuka (1999a,b) have shown that the fragmentation of a rotating collapsing core into a multiple system is difficult in the isothermal stage. Matsumoto and Hanawa (2003) have extended the collapse calculation by using a nested-grid hydro code and a simplified barotropic equation of state that mimics the thermal evolution, and have shown that the first-core disk increases the rotation-to-gravitational energy ratio ( $T/|W|$ ) by mass accretion. A stability analysis of a rotating polytropic gas shows that gas with  $T/|W| > 0.27$  is unstable for non-axisymmetric perturbations (e.g., Imamura *et al.* 2000). If the first-core disk rotates fast enough that the angular speed  $\times$  the free-fall time satisfies  $\Omega_c(4\pi G \rho_c)^{-1/2} \gtrsim (0.2 - 0.3)$ , fragments appear and grow into binaries and multiples in the first core phase. The non-axisymmetric nonlinear spiral pattern can transfer the angular momentum of the accreting gas.

### 3.3. Magnetic Fields

Detailed self-consistent calculations accounting for both thermal and magnetic support (Mouschovias and

Spitzer, 1976; Tomisaka *et al.*, 1988) show that the maximum stable mass can be expressed as  $M_{\text{mag,max}} \sim M_{\text{BE}} \left\{ 1 - [0.17/(G^{1/2} M/\Phi)_c]^2 \right\}^{-3/2}$ , where  $(M/\Phi)_c$  is the central mass-to-flux ratio and  $M_{\text{BE}} = 1.18 c_s^4 / G^{3/2} p_{\text{ext}}^{1/2}$  is the Bonnor-Ebert mass (Bonnor, 1956, 1957; Ebert, 1957). A similar formula was proposed by McKee (1989),  $M_{\text{mag,max}} \sim M_{\text{BE}} + \Phi_B / 2\pi G^{1/2}$ .

Further support is provided by rotation. For a core with specific angular momentum  $j$ , the maximum stable mass is given by  $M_{\text{max}} \sim [M_{\text{mag,max}}^2 + (4.8 c_s j / G)^2]^{1/2}$  (Tomisaka *et al.*, 1989). The dynamical runaway collapse begins when the core mass exceeds this maximum stable mass (magnetically supercritical cloud). Quasi-static equilibrium configurations exist for cores less massive than the maximum stable mass. The evolution of these subcritical cores is controlled by the processes of ambipolar diffusion and magnetic braking, both of which have longer timescales than the gravitational free fall. As the core contracts, the density grows and, when  $n \gtrsim 10^{12} \text{ cm}^{-3}$ , the magnetic field is effectively decoupled from the gas. At these densities, Joule dissipation becomes important and particle drifts are qualitatively different from ambipolar diffusion (Nakano *et al.*, 2002).

The magnetic field is also responsible for the transfer of angular momentum in magnetized rotating cores, by a process called magnetic braking. Magnetic braking is caused by the azimuthal component of the Lorentz force  $(\vec{j} \times \vec{B})_\phi$ . In the evolution of subcritical cores, the magnetic braking is important during the quasi-static contraction phase controlled by the ambipolar diffusion (Basu and Mouschovias, 1994). In the dynamical runaway collapse, the rotational speed is smaller than the inflow speed (Tomisaka, 2000)

### 3.4. Outflows

The magnetic field generates an outflow, by which star forming gas loses its angular momentum and accretes onto a protostar. Magneto-hydrodynamical simulations of the contraction of molecular cores (Tomisaka, 1998, 2000, 2002; Allen *et al.*, 2003; Banerjee and Pudritz, 2006) have shown that after the formation of the first core, the gas rotates around the core, a toroidal magnetic field is induced and magnetic torques transfer angular momentum from the disk midplane to the surface. Outflows are accelerated in two ways: i) The gas which has received enough angular momentum compared with the gravity is ejected by the excess centrifugal force (magnetocentrifugal wind mechanism; Blandford and Payne, 1982). ii) In a core with a weak magnetic field, the magnetic pressure gradient of the toroidal magnetic field accelerates the gas and an outflow is formed in the direction perpendicular to the disk.

Axisymmetric 2D simulations show that i) at least 10% of the accreted mass is ejected; ii) the angular momentum is reduced to a factor  $10^{-4}$  of the value of the parent cloud at the age of  $\simeq 7000$  yr from the core formation. This resolves the angular momentum problem (Tomisaka, 2000). 7000 yr

from the first core formation, the mass of the core reaches  $\sim 0.1M_{\odot}$  and the outflow extends to a distance from the core of  $\simeq 2000$  AU with a speed of  $\sim 2 \text{ km s}^{-1}$  (Tomisaka, 2002). If the accretion continues and the core mass grows to one solar mass, the outflow expands and its speed is further increased. It should be noted that the outflow refers to the physics of the first core collapse only; the energetics of outflows during the second core collapse phase are yet to be determined.

### 3.5. Radiative Transfer in Multi-Dimensions

Radiation transport has been shown to play a significant role in the outcome of fragmentation into binary and multiple systems (Boss *et al.*, 2000; Whitehouse and Bate, 2005) and in limiting the largest stellar mass in 2D (Yorke and Sonnhalter, 2002) and 3D simulations (Edgar and Clarke, 2004; Krumholz *et al.*, 2005c). The strong dependence of the evolution of isothermal and nonisothermal cloud models on the handling of the cloud's thermodynamics implies that collapse calculations must treat the thermodynamics accurately in order to obtain the correct solution (Boss *et al.*, 2000). Because of the great computational burden imposed by solving the mean intensity equation in the Eddington approximation (the computational time is increased by a factor of 10 or more) it is tempting to sidestep the Eddington approximation solution altogether and employ a simple barotropic prescription (e.g., Boss, 1981; Bonnell, 1994; Bonnell and Bate, 1994a; Burkert *et al.*, 1997; Klein *et al.*, 1999). However, Boss *et al.* (2000) showed that a simple barotropic approximation is insufficient and radiative transfer must be used. We discuss the various methods of radiation transport in section 3.b.6.

## 4. METHODOLOGY OF NUMERICAL SIMULATIONS

### 4.1. Complexity of the Problem of Low Mass Star Formation

The computational challenge for simulations of low mass star formation is that star formation occurs in clouds over a huge dynamic range of spatial scales, with different physical mechanisms being important on different scales. The gas densities in these clouds also varies over many orders of magnitude as a result of supersonic turbulence and gravitational collapse. Gravity, turbulence, radiation and magnetic fields all contribute to the star formation process. Thus the numerical problem is multi-scale, multi-physics and highly non-linear. To develop a feel for the range of scale a simulation must cover, we can consider the internal structure of GMCs as hierarchical, consisting of smaller subunits within larger ones (Elmegreen and Falgarone, 1996). GMCs vary in size from 20 to 100 pc., in density from 50 to 100  $\text{H}_2 \text{ cm}^{-3}$  and in mass from  $10^4$  to  $10^6 M_{\odot}$ .

Self-gravity and turbulence are equally important in controlling the structure and evolution of these clouds. Magnetic fields are likely to play an important role as well (Heiles *et al.*, 1993; McKee *et al.*, 1993). Embedded within the GMCs are dense clumps that may form clusters of stars. These clumps are few pc. in size, have masses of a few thousand  $M_{\odot}$  and mean densities  $\sim 10^3 \text{ H}_2 \text{ cm}^{-3}$ . The clumps contain dense cores with radii  $\sim 0.1$  pc., densities  $10^4$ - $10^6 \text{ H}_2 \text{ cm}^{-3}$  and masses ranging from 1 to several  $M_{\odot}$ . These cores likely form individual stars or low order multiple systems. The role of turbulence and magnetic fields in the fragmentation of molecular clouds has been investigated by 3D numerical simulations (e.g., Padoan and Nordlund, 1999; Ostriker *et al.*, 1999; Ballesteros-Paredes, 2003; Mac Low and Klessen, 2003; Nordlund and Padoan, 2003).

A simulation that starts from a region of a turbulent molecular clouds ( $R \sim$  few pc.) and evolves through the isothermal core collapse into the formation of the first hydrostatic core at densities of  $10^{13} \text{ H}_2 \text{ cm}^{-3}$  requires an accurate calculation across 10 orders of magnitude in density and 4-5 orders of magnitude in spatial scale. To resolve 100 AU separation binaries, one needs a resolution of about 10 AU. To follow the collapse all the way to an actual star would require a further 10 orders of magnitude increase in density and 2-3 more orders of magnitude in spatial scale. Such extraordinary computational demands rule out fixed grid simulations entirely and can be addressed only with accurate AMR or SPH approaches.

### 4.2. Smooth Particle Hydrodynamics

The description of the gravitational collapse requires a large dynamic range of spatial resolution. An efficient way to achieve this is to use Lagrangian methods. Smoothed particle hydrodynamics (SPH) is a fully Lagrangian particle method designed to describe compressible fluid dynamics. This method is economical in handling hydrodynamic problems that have large, almost empty regions. A variety of astrophysical problems including star formation have been studied with SPH, because of its simplicity in programming two- and three-dimensional codes and its versatility to incorporate self-gravity. A broad discussion of the method can be found in a review by Monaghan (1994). An advantage of SPH is its conservation property; SPH is Galilean invariant and, in contrast to grid-based methods, conserves both linear and angular momentum simultaneously. The method to conserve the total energy within a computer round-off-error is explained in Inutsuka (2002). In order to further increase the dynamic range of spatial resolution, Kitsionas and Whitworth (2002) introduced particle splitting, which is an adaptive approach in SPH.

The “standard” SPH formalism adopts artificial viscosity that mimics the classical von-Neumann Richtmeyer viscosity. This tends to give poor performance in the description of strong shocks. In two- or three-dimensional calculations of colliding streams, standard SPH particles often

penetrate into the opposite side. This unphysical effect can be partially eliminated by the so called XSPH prescription (*Monaghan*, 1989), which does not introduce the (required) additional *dissipation*, but results in additional *dispersion* of the waves. As a more efficient method for handling strong shocks in the SPH framework, the so called “Godunov SPH” was proposed by *Inutsuka* (2002), who implemented the exact Riemann solver in the strictly conservative particle method. This was used in the simulation of the collapse and fragmentation of self-gravitating cores (*Tsuribe and Inutsuka*, 1999a; *Cha and Whitworth*, 2003a,b).

The implementation of self-gravity in SPH is relatively easy and one can use various acceleration methods, such as *Tree-Codes*, and special purpose processors (e.g., GRAPE board). The flux-limited diffusion radiative transfer was recently incorporated in SPH by *Whitehouse and Bate* (2004), *Whitehouse et al.* (2005) and *Bastien, Cha, and Viau* (2004).

Several groups are now using “sink particles” to follow the subsequent evolution even after protostars are formed (*Bate et al.*, 1995). This is a prescription to continue the calculations without resolving processes of extremely short timescale around stellar objects. *Krumholz et al.*, (2004) have introduced sink particles for the first time into Eulerian grid-based methods and in particular for AMR.

### 4.3. Fixed-Grid Hydrodynamics

Since the time of its introduction, the numerical code of choice for supersonic hydrodynamic turbulence has been the Piecewise Parabolic Method (<http://www.lcse.umn.edu/>) (PPM) of *Colella and Woodward* (1984). PPM is based on a Riemann solver (the discretized approximation to the solution is locally advanced analytically) with a third order accurate reconstruction scheme, which allows an accurate and stable treatment of strong shocks, while maintaining numerical viscosity to a minimum away from discontinuities. Because the physical viscosity is not explicitly computed (PPM solves the Euler equations), large scale PPM flows are characterized by a very large effective Reynolds number (*Porter and Woodward*, 1994). Direct numerical simulations (DNS) of the Navier-Stokes equation, where the physical viscosity is explicitly computed, require a linear numerical resolution four times larger than PPM to achieve the same wave-number extension of the inertial range of turbulence as PPM (*Sytnik et al.*, 2000). From this point of view, therefore, PPM has a significant advantage over DNS codes. Furthermore, DNS codes are generally designed for incompressible turbulence, and hence of limited use for simulations of the ISM.

Codes based on straightforward staggered mesh finite difference methods, rather than Riemann solvers, have also been used in applications to star formation and interstellar turbulence, such as the Zeus code (<http://cosmos.ucsd.edu/>) (*Stone and Norman*, 1992a,b) and the Stagger Code ([www.astro.ku.dk/StaggerCode/](http://www.astro.ku.dk/StaggerCode/)) (*Nordlund and Galsgaard*, 1995; *Gudiksen and Nordlund*, 2005). Finite dif-

ference codes address the problem of supersonic turbulence with the introduction of localized numerical viscosity to stabilize the shocks while keeping viscosity as low as possible away from shocks. The main advantage of this type of code, compared with Riemann solvers, is their flexibility in incorporating new physics and their computational efficiency.

Fixed-grid codes cannot achieve the dynamical range required by problems involving the gravitational collapse of protostellar cores. Such problems are better addressed with particle methods such as SPH, or by generalizing the methods used for fixed-grid codes into AMR schemes. The main advantage of large fixed-grid experiments is their ability to simulate the physics of turbulent flows. As supersonic turbulence is believed to play a crucial role in the initial fragmentation of star-forming clouds, fixed-grid codes may still be the method of choice to generate realistic large scale initial conditions for the collapse of protostellar cores. Recent attempts of simulating supersonic turbulence with AMR methods are promising (*Kritsuk et al.*, 2006), but may be truly advantageous only at a resolution above  $\sim 1,000^3$ . SPH simulations to date have resolution far too small for the task, as commented above, and have not been used so far as an alternative method to investigate the physics of turbulence.

### 4.4. Adaptive Mesh Refinement Hydrodynamics and Nested Grids

The adaptive mesh refinement (AMR) scheme utilizes underlying rectangular grids at different levels of resolution. Linear resolution varies by integral refinement factors between levels, and a given grid is always fully contained within one at the next coarser level (excluding the coarsest grid). The origin of the method stems from the seminal work of *Berger and Oliger* (1984) and *Berger and Colella* (1989). The AMR method dynamically resizes and repositions these grids and inserts new, finer ones within them according to adjustable refinement criteria, such as the numerical Jean’s condition (*Truelove et al.*, 1997). Fine grids are automatically removed as flow conditions require less resolution. During the course of the calculation, some pointwise measure of the error is computed at frequent intervals, typically every other time step. At those times, the cells that are identified are covered by a relatively small number of rectangular patches, which are refined by some even integer factor.

Refinement is in both time and space, so that the calculation on the refined grids is computed at the same Courant number as that on the coarse grid. The finite difference approximations on each level of refinement are in conservation form, as is the coupling at the interface between grids at different levels of refinement. AMR has three substantial advantages over standard SPH. Combined with high order Godunov methods, AMR achieves a much higher resolution of shocks. This is important in obtaining accuracy in supersonic turbulent flows in star forming clumps and cores and

in accretion shocks onto forming protostars. AMR allows high resolution at *all* points in the flow as dictated by the physics. Unlike SPH, where particles are taken away from low density regions, where accuracy is lost, and concentrated into high density regions, AMR maintains high accuracy everywhere. An important consequence of this is that if SPH were to maintain the same comparable resolution as AMR everywhere in the flow, it would be prohibitively expensive. AMR is based on fixed Eulerian grids and thus can take advantage of sophisticated algorithms to incorporate magnetic fields and radiative transfer. This is far more difficult in a particle-based scheme. AMR was first introduced into astrophysics by *Klein et al.* (1990, 1994) and has been used extensively both in low mass and high mass star formation simulations (*Truelove et al.*, 1998; *Klein*, 1999; *Klein et al.*, 2000, 2003, 2004a; *Krumholz et al.*, 2005c).

An advantage of SPH over *Cartesian* grid based AMR is that for pure hydrodynamics it can conserve both linear and angular momentum simultaneously to within round-off errors whereas *Cartesian* grid based AMR cannot. However, if one uses a cylindrical or spherical coordinate system for the simulation of protostellar disks for instance, then grid based AMR conserves total angular momentum to round-off. We point out, however, that these statements apply only to pure hydrodynamics. Once forces such as gravity are included, the situation becomes worse and both grid codes that solve the Poisson equation or SPH codes that use tree-type acceleration or grid based methods for gravity lose the conservation property for total linear momentum as well.

There are several ways to implement AMR. They can be broadly divided into two categories: Meshes with fixed number of cells, such as in Lagrangian or rezoning approaches, and meshes with variable number of cells, such as unstructured finite elements, structured cell-by-cell and structured sub-grid blocks. For various reasons the most widely adopted approaches in astrophysics are structured sub-grid blocks and cell-by-cell. The first was developed by *Berger and Oliger* (1984) and *Berger and Colella* (1989). It is used in the AMR code ORION developed by Klein and collaborators (*Klein*, 1999; *Crockett et al.*, 2005) and in the community code ENZO (*Norman and Bryan*, 1999). The cell-by-cell approach such as in PARAMESH (Mac-Neice et al., 2000) is used in the community code Flash (*Banerjee et al.*, 2004). A hybrid approach is used in the code NIRVANA (*Ziegler*, 2005). The cell-by-cell method has the advantages of flexible and efficient refinement patterns and low memory overhead and the disadvantages of expensive interpolation and derivation formulas and large tree data structures. The sub-grid block method is more efficient and more suitable for shock capturing schemes than the cell-by-cell method, at the price of some memory overhead.

Finally, nested grids consisting of concentric hierarchical rectangular subgrids can also be very effective for problems of well defined geometry (*Yorke et al.*, 1993). These methods are advantageous for tracing the non-homologous runaway collapse of an initially symmetrical cloud in which

the coordinates of a future dense region are known in advance (*Tomisaka*, 1998). The finest subgrid is added dynamically when spatial resolution is needed as in AMR methods.

#### 4.5 Approaches for Magneto-Hydrodynamics

Since strong shocks often appear in the astrophysical phenomena, a shock-capturing scheme is needed also in MHD. Upwind schemes based on the Riemann solver are used as the MHD engine. Schemes well known in hydrosimulations, such as Roe's approximate Riemann solver (*Brio and Wu*, 1988; *Ryu and Jones*, 1995; *Nakajima and Hanawa*, 1996), piecewise parabolic method (PPM; *Dai and Woodward*, 1994), are also applicable to MHD.

Special attention should be paid to guarantee  $\text{div} \vec{B} = 0$  in MHD simulations. To ensure that the divergence of Maxwell stress tensor  $T_{ij} = -(1/4\pi)B_iB_j + (1/8\pi)B^2\delta_{ij}$  gives the Lorentz force, the first term of right-hand side  $\partial_j(B_iB_j)$  must be equal to  $B_j\partial_jB_i$ . This requires  $B_i\partial_jB_j = 0$  and means that a fictitious force appears along the magnetic field if the condition of divergence-free is broken. The divergence of the magnetic field amplifies the instability of the solution even for a linear wave. Thus, it is necessary for the MHD scheme to keep the divergence of the magnetic field zero within a round-off error or at least small enough. This divergence-free nature should be satisfied for the boundaries of subgrids in AMR and nested grid schemes.

One solution is based on “constrained transport (CT)” (*Evans and Hawley* 1988), in which the staggered collocation of the components of magnetic field on the cell faces makes the numerical divergence vanish exactly. In the staggered collocation, the electric field  $-\vec{v} \times \vec{B}$  of the induction equation  $\partial_t \vec{B} = \nabla \times (\vec{v} \times \vec{B})$  is evaluated on the edge of the cell-face and the line integral along the edge gives the time difference of a component of the magnetic field. Note that the electric field on one edge appears twice to complete the induction equation. To guarantee a vanishing divergence of the magnetic field, CT requires the two evaluations to coincide with each other.

To utilize the Godunov-type Riemann solver in the context of CT, *Balsara and Spicer* (1999) proposed a scheme as follows: (1) face-centered magnetic field is interpolated to the cell center; (2) from the cell-centered variables, the numerical flux at the cell face is obtained using a Riemann solver; (3) the flux is interpolated to the edge of the cell-face and the electric field in the induction equation is obtained; (4) new face-centered magnetic field is obtained from the induction equation. Variants of this method are widely used [see also *Ryu et al.*, (1998) and *Ziegler*, (2004)].

Avoiding staggered collocation of the magnetic field requires divergence cleaning. In this case, divergence cleaning is realized by replacing the magnetic field every step as  $\vec{B}^{new} = \vec{B} - \vec{\nabla}\vec{\Phi}$ , where  $\vec{\nabla}^2\vec{\Phi} = \text{div} \vec{B}$  (Hodge projection), or by solving a diffusion equation for  $\text{div} \vec{B}$  as  $\partial_t \vec{B} = \eta \vec{\nabla}(\vec{\nabla} \cdot \vec{B})$ . The former is combined with pure

Godunov-type Riemann solvers using only cell-centered variables (Ryu *et al.*, 1995). Crockett *et al.* (2005) reported that the divergence cleaning of the face-centered magnetic field appearing in the numerical flux based on an unsplit, cell-centered Godunov scheme improves its accuracy and stability.

Powell *et al.* (1999) proposed a different formalism, in which  $\text{div } \vec{B}$  term is kept in the MHD equations as a source (e.g., the Lorentz force  $(\nabla \times \vec{B}) \times \vec{B}/4\pi$  gives an extra term related to  $\text{div } \vec{B}$  as  $-\vec{B} \nabla \cdot \vec{B}$  besides the Maxwell stress tensor term  $-T_{ij}$ , in the equation for momentum density.) In this formalism,  $\text{div } \vec{B}$  is not amplified but advected along the flow. Comparison between various methods is found in Tóth (2000), Dedner *et al.* (2002), Balsara and Kim (2004) and Crockett *et al.* (2005).

There have been attempts to solve the induction equation with SPH methods (e.g., Stellingwerf and Peterkin, 1994; Byleveld and Pongracic, 1996; Price and Monaghan, 2004a,b,c, 2005). A major obstacle is an instability that develops when the momentum and energy equations are written in conservation form. As a result, the equations must be written in a way that does not conserve momentum (Phillips and Monaghan, 1985; Morris, 1996), which is a major concern for the accurate treatment of shocks. Results of recent tests of the state-of-the-art SPH MHD code (Price and Monaghan, 2004c) appear to be rather poor even for very mild shocks, and we conclude that MHD with SPH is not yet viable for simulations.

#### 4.6. Approaches for Radiation Transport

Several levels of approximation of the radiation transport in star formation simulations can be used and details of various methods can be found in Mihalas and Mihalas (1984) and Castor (2004). Here we briefly describe these methods and point out their strengths and weaknesses. Although modern simulations using radiative transfer are still at an early stage, we include methods that hold promise for the future that will circumvent the weaknesses of more approximate approaches currently in place.

The simplest improvement beyond a barotropic stiffened EOS is the diffusion approximation which pertains to the limit in which radiation can be treated as an ideal fluid with small corrections. The approximation holds when the photon mean free path is small compared with other length scales. The combined energy equation for the gas and radiation results in an implicit non-linear diffusion equation for the temperature. The weakness of the diffusion approximation is that it is strictly applicable to optically thick regimes and performs poorly in optically thin regions. This can be severe in optically thin regions of an inhomogeneous turbulent core or in the optically thin atmosphere surrounding a developing protostar.

The next level of approximation is the Eddington approximation (Boss and Myhill, 1992; Boss *et al.*, 2000). It can be shown that the diffusion approximation leads directly to Eddington's approximation  $P_\nu = \frac{1}{3} E_\nu I$ , where  $P_\nu$

is the pressure tensor moment of the specific intensity of radiation,  $E_\nu$  is the scalar energy density of radiation and  $I_\nu$  is the isotropic identity tensor. This approximation, coupled with dropping the time dependent term in the 2nd moment equation of transfer results in a combined parabolic 2nd order time dependent diffusion equation for the energy density of the radiation field. This formulation of the Eddington approximation is used in Boss *et al.* (2000). The approximation results in a loss of the finite propagation speed of light  $c$  and a loss of the radiation momentum density, thus there is an error in the total momentum budget. In optically thin regions, the radiation flux can increase without limit. As with all diffusion like methods, this approach also suffers from shadow effects whereby radiation will tend to fill in behind optically thick structures and may lead to unphysical heating.

An alternative approach is the Flux Limited Diffusion (FLD), that modifies the Eddington approximation, and compensates for the errors made in dropping the time dependent flux term by including a correction factor in the diffusion coefficient for the radiation flux. This correction factor, called a flux limiter, is in general a tensor and has the property that the flux goes to the diffusion limit at large optical depth and it correctly limits the flux to be no larger than  $cE$  in the optically thin regime. This improvement over the Eddington approximation has been used by Klein *et al.* (2004c) for the simulation of both low mass and high mass star formation. The resulting sparse matrices introduced by the diffusion like terms are solved by multi-grid iterative methods in an AMR framework. The flux-limiting correction can cause errors of order 20 in the flux-limiter (or the flux), similar to the errors of the Eddington approximation of 20% in the Eddington factor at  $\tau = 0$  in the Milne problem (Castor 2004). The FLD method's also suffer from shadow effects which can be severe.

The next level of approximation, the variable Eddington tensor method, removes many of the inaccuracies of the Eddington approximation and the flux limiter modification. It was first formulated in multi-dimensions for astrophysical problems by Dykema *et al.* (1996). In essence, if the precise ratio of the pressure tensor to the energy density were included as an ad hoc multiplier in the Eddington approximation equations they would represent an exact closure of the system. The tensor ratio is obtained iteratively from either an auxiliary solution of the exact transport equation for the specific intensity or using an approximate analytic representation of the tensor. This method holds promise for future simulations, but has yet to be used in star formation.

The final two approaches, which are highly accurate and deal with the angle dependent transport equation directly, are  $S_N$  methods and Monte Carlo methods. They have not yet been developed for simulations in star formation because the cost in 3D is prohibitive. The  $S_N$  method is a short characteristic method in which a bundle of rays is created at every mesh point and are extended in the upwind direction only as far as the next spatial cell. The main problem is in finding the efficient angle set to represent the radiation

field in 2 or 3 dimensions (*Castor*, 2004). Finally, one might consider Monte Carlo methods to solve the transport equation. Although simple to implement (its great advantage), this method suffers from needing a vast number of operations per timestep to get accurate statistics in following the particles used to track the radiation field. Both of these methods will avoid shadow effects and may be necessary to accurately treat optically thick inhomogeneous structures that form in accretion flows onto protostars.

Radiative transfer implementations have recently been developed also for SPH methods, based on the flux-limited diffusion (*Whitehouse et al.*, 2005) or the Monte Carlo method (*Stamatello and Whitworth*, 2003, 2005).

#### 4.7. Comparison of Computational Methods

Based on the physical processes and numerical methodologies discussed in the previous sections we can compare numerical schemes according to their ability to handle the following problems both accurately and efficiently: (a) turbulence, (b) strong shocks, (c) self-gravity, (d) magnetic fields, (e) radiative transfer.

The standard SPH method has been successful with (c) and implementations of (e) have been recently developed in the flux-limited diffusion approximation and with a Monte Carlo method. It does not include (d), it is well known to be inadequate for (b) and has had virtually no applications to (a) to date. As any Lagrangian particle methods, SPH provides good resolution in high density regions, but very poor in low density ones. The Godunov SPH method improves the standard SPH codes because of its ability to address (b), but does not provide a solution to (d) and is untested for (a) as well. Although MHD is currently under development in SPH, results of standard MHD tests with a state-of-the-art code show the need for significant improvements even in the case of very mild shocks. Current applications of SPH should therefore be limited to non-MHD problems and the accuracy and performance of SPH with turbulent flows must be thoroughly tested.

In hydrodynamical problems, grid-based methods such as MUSCL (*van Leer*, 1979) and PPM (*Colella and Woodward*, 1984) use exact Riemann Solvers to construct the numerical fluxes and provide very accurate description in astrophysical flows with strong shocks (b). They have also been thoroughly tested with compressible turbulent flows, and MHD versions have been developed that can address both (d) and (e). Traditional finite-difference grid-based schemes may still be useful, because the best of them can also accurately address (a), (b), (d) and (e), at a lower cost of code development and computer resources. Point (c) can also be efficiently dealt with by grid-based codes thanks to AMR methods. However, the development of AMR schemes that satisfy (c) and at the same time (d) has begun only recently. These schemes exist and have been successfully tested, but it is unclear at present which approach will provide the best trade off between accuracy and performance.

The constrained transport method appears to be the ideal one to guarantee the  $\nabla \cdot B = 0$  condition. Various schemes have been proposed even in the category of Godunov-type methods with a linearized Riemann Solver. An exact MHD Riemann Solver would be more adequate to handle strong shocks, but it is not available yet. In MHD we have to solve seven characteristics even in one-dimensional problems, which hinders an efficient construction of numerical fluxes based on the non-linear waves. Furthermore, the discovery of the existence of the MHD intermediate shocks (*Brio and Wu*, 1988) brings an additional difficulty in the categorization and prediction of the emerging non-linear waves. Among possible solutions, a linearized Riemann Solver with artificial viscosity may still be a useful option.

The Godunov MHD code of *Crockett et al.* (2005) has been merged with the AMR RHD code of *Klein et al.* (2004a,b) into the first fully developed AMR magneto-radiation-hydrodynamic code (ORION) to be used in simulations of star formation capable of addressing (a) through (e).

### 5. RECENT SIMULATIONS AND CONFRONTATION WITH THE OBSERVATIONS

#### 5.1. Turbulent Fragmentation of Molecular Clouds

The fragmentation of molecular clouds is the result of a complex interaction of supersonic turbulence with gravity and magnetic fields. Supersonic turbulent flows generate nonlinear density enhancements through a complex network of interacting shocks. Some density enhancements are massive and dense enough to undergo gravitational instability and collapse into stars. A fundamental problem with our understanding of star formation is that the physics of turbulence is not fully understood. In order to investigate the process of turbulent fragmentation we must rely on large numerical simulations that barely resolve the scale-free nature of interstellar turbulent flows. If the scaling laws of turbulence play a role in the star formation process, we cannot accurately test their effects numerically, unless those scaling laws are well reproduced in the simulations. *Ballesteros-Paredes et al.* (2006) have tested the idea that the power spectrum of turbulence determines the Salpeter IMF (*Padoan and Nordlund*, 2002). However, their simulations do not generate a turbulence inertial range, due to the combined effect of low resolution and large numerical diffusivity. Their velocity power spectra do not show any extended power laws, and they even differ between their grid and SPH simulations. As a consequence, such numerical simulations fail to reproduce a scale free mass distribution of unstable cores.

Other recent SPH simulations have been used to compute the stellar mass distribution (e.g., *Bonnell et al.*, 2003; *Klessen*, 2001) and to test the effect of turbulence on star formation (*Delgado-Donate et al.*, 2004). Although such SPH simulations are ideally suited to follow the collapse of individual objects due to their Lagrangian nature, their size

is far too small to generate an inertial range of turbulence, as discussed in section 3.a.1.

Despite their limitations, numerical simulations carried out over the last few years have given us a good statistical picture of the process of fragmentation of magnetized supersonic flows. The following are the most important results: i) The dissipation time of turbulence is almost independent of the magnetic field strength. The turbulence decays in approximately one dynamical time in both equipartition and super-Alfvénic flows (Padoan and Nordlund, 1997; MacLow *et al.*, 1998; Stone *et al.*, 1998; Padoan and Nordlund, 1999; Biskamp and Muller, 2000). ii) The velocity power spectrum and structure functions are power laws over an inertial range of scales (Boldyrev, 2002; Boldyrev *et al.* 2002a,b; Padoan *et al.*, 2004b). In the limit of very large rms Mach number, the turbulent velocity power spectrum scales approximately as  $u_k^2 \propto k^{-1.8}$  and the velocity structure functions follow the relative scaling predicted by Boldyrev (2002). For intermediate levels of compressibility, the scaling exponents depend on the rms Mach number (Padoan *et al.*, 2004b). iii) The power spectrum of the gas density is a power law over an inertial range of scales. Its slope is a function of the rms Mach number of the flow and of the average magnetic field strength (Padoan *et al.*, 2004b; Beresnyak *et al.*, 2005). iv) With an isothermal equation of state, the probability density function of gas density is well approximated by a Log-Normal distribution (Vazquez-Semadeni, 1994; Padoan *et al.*, 1997; Scalo *et al.*, 1998; Passot and Vazquez-Semadeni, 1998; Nordlund and Padoan, 1999; Ostriker *et al.*, 1999; Wada and Norman, 2001), with the dispersion of linear density proportional to the rms Mach number of the flow (Padoan *et al.*, 1997; Nordlund and Padoan, 1999; Ostriker *et al.*, 1999; Li *et al.*, 2004). v) If the kinetic energy exceeds the magnetic energy, the distribution of the magnetic field strength,  $B$ , is very intermittent and is correlated with the gas density,  $n$ . The scatter plot of  $B$  versus  $n$  shows a very large dispersion and a well defined power law upper envelope (Padoan and Nordlund, 1999; Ostriker *et al.*, 2001). If the kinetic energy is comparable to the magnetic energy, strong density enhancements are still possible in the direction of the magnetic field, but fluctuations of  $B$  are small and independent of  $n$ . vi) The flow velocity is correlated to the gas density. Because density is increased by shocks, where the velocity is dissipated, dense filaments and cores have lower velocity than the low density gas (Padoan *et al.*, 2001b). vii) The mass distribution of gravitationally unstable turbulent density peaks is very close to the stellar IMF and follows the analytical model of Padoan and Nordlund (2002) (Li *et al.*, 2004; Tilley and Pudritz, 2004).

There is now substantial observational evidence indicating that these main properties of supersonic MHD turbulence are indeed found in molecular clouds. The comparison of numerical simulations of turbulence with observational data was pioneered by Falgarone *et al.* (1994) and continued by many others (e.g., Padoan *et al.* 1998, 1999; Padoan *et al.* 2001a,b; Ostriker *et al.*, 2001; Ballesteros-

Paredes and Mac Low, 2002; Ossenkopf, 2002; Padoan *et al.*, 2004a; Gammie *et al.*, 2003; Klessen *et al.*, 2005; Esquivel and Lazarian, 2005).

However, with the exception of several works by Padoan *et al.* and the work of Ossenkopf (2002), where post-processed three dimensional non-LTE radiative transfer calculations were carried out, all other studies are based on a simple comparison of density and velocity fields in the simulations with the observed quantities. Some recent works addressing the comparison of turbulence simulations and observational data include studies of velocity scaling, showing that molecular cloud turbulence is driven on large scale (e.g., Ossenkopf and Mac Low, 2002; Heyer and Brunt, 2004) and studies of core properties, showing that turbulent flows naturally generate dense cores with shapes, internal turbulence, rotation velocity and magnetic field strength consistent with the observations (e.g., Padoan and Nordlund, 1999; Gammie *et al.*, 2003; Tilley and Pudritz, 2004; Tilley and Pudritz, in preparation; Li *et al.*, 2004).

## 5.2. Collapse and Fragmentation of Molecular Cloud Cores into Low-Mass Stars

Over the past several years two dominant models of how stars acquire their final mass have emerged: Direct Gravitational Collapse and Competitive Accretion. In both theories, a star initially forms when gravitational bound gas collapses. In the gravitational collapse scenario, after a protostar has consumed or expelled all the gas in its initial core, it may continue accreting from the parent clump, but it will not significantly alter its mass (McKee and Tan, 2003; Padoan *et al.*, 2005; Krumholz *et al.*, 2005b). Competitive accretion, in contrast, requires that the amount accreted after consuming the initial core be substantially larger than the protostellar mass.

Krumholz *et al.* (2005a) define  $f_m \equiv \dot{m}_* t_{dyn}/m_*$  as the fractional change in mass that a protostar of mass  $m_*$  undergoes each dynamical time  $t_{dyn}$  of its parent clump, starting after the initial core has been consumed by the accreting protostar. Gravitational collapse theory suggests that  $f_m \ll 1$ , while competitive accretion requires  $f_m \gg 1$ . In recent work examining the plausibility of competitive accretion, Krumholz *et al.* (2005a) considered two possible scenarios. In the first scenario, the gas the protostar is accreting is not accumulated into bound structures on scales smaller than the entire clump. For unbound gas, self-gravity may be neglected and the entire problem can be treated as Bondi-Hoyle accretion in a turbulent medium of non-self-gravitating gas onto a point particle. In a companion paper (Krumholz *et al.*, 2006) they develop the theory for Bondi-Hoyle accretion in a turbulent medium. Using this theory they derive the accretion rate for such a turbulent medium and they confirm their theory with detailed, high resolution, converged AMR simulations. By using this accretion rate and the definition of the virial parameter,  $\alpha_{vir} \equiv M_{vir}/M$ , and the dynamical time,  $t_{dyn} \equiv R/\sigma$ , where  $\sigma$  is the velocity dispersion in the gas, they show that the accretion of un-

bound gas gives  $f_{\text{m-BH}} = (14.4, 3.08\frac{L}{R})\phi_{\text{BH}}\alpha_{\text{vir}}^{-2}(\frac{m_*}{M})$  for a (spherical, filamentary) star-forming region, where  $\phi_{\text{BH}}$  represents the effects of turbulence (Krumholz *et al.*, 2005a).

From this it is clear that competitive accretion is most effective in low mass clumps with virial parameters  $\alpha_{\text{vir}} \ll 1$ . They then examined the observed properties of a large range of star forming regions spanning both low mass and high mass stars and computed the properties for each region yielding  $\alpha_{\text{vir}}$ ,  $\phi_{\text{BH}}$  and  $f_{\text{m-BH}}$ . In virtually every region examined, the virial parameter  $\alpha_{\text{vir}} \sim 1$  and  $f_{\text{m-BH}} \ll 1$ . Thus *none* of the star-forming regions are consistent with competitive accretion, but all are consistent with direct gravitational collapse. *Edgar and Clarke*, (2004) examined Bondi-Hoyle accretion onto stars including radiation pressure effects and found that radiation pressure halts further accretion around stars more massive than  $\sim 10M_{\odot}$ . It is important to point out that while this result may be true for accretion of unbound gas onto a point particle, it is not true for global collapse and accretion from a bound core as shown in more realistic full 3D radiation hydrodynamics simulations by Krumholz *et al.* (2005c), who form massive stars with  $M \sim 40M_{\odot}$ . If *Edgar and Clarke*'s results do hold for Bondi-Hoyle accretion (but not accretion from a core), then the only way for massive stars to grow in competitive accretion is by direct collisions. This requires densities of  $10^8 \text{ pc}^{-3}$ ,  $\sim 3$  orders of magnitude larger than any observed in the galactic plane. Furthermore, no competitive accretion model to date has included the effects of radiation pressure; a glaring omission if the model is attempting to explain high mass stars. It follows that competitive accretion is not a viable mechanism for producing the stellar IMF.

In a second possible competitive accretion scenario, Krumholz *et al.* (2005a, supplemental section) examined another way that a star could increase its mass by capturing and accreting other gravitationally bound cores. Their theory results in the calculation of  $f_{\text{m-cap}}$ , the fractional change in mass that a protostar undergoes by capturing bound cores. As found with  $f_{\text{m-BH}}$ , all the values are estimated to be three more orders of magnitude below unity and again, competitive accretion is found not to work.

If competitive accretion is clearly not supported by observations in any known star forming region, why do the simulations (Bonnell *et al.*, 1998, 2001; Bate *et al.*, 2005) almost invariably find competitive accretion to work? Is there a fundamental flaw in the methodology used in competitive accretion scenarios (SPH) or is the problem one of physics and initial conditions? As Krumholz *et al.* (2005a) point out, all competitive accretion have virial parameters  $\alpha_{\text{vir}} \ll 1$ . Some of the simulations start with  $\alpha_{\text{vir}} \approx 0.01$  as a typical choice (Bonnell *et al.*, 2001a,b; Klessen and Burkert, 2000, 2001). For other simulations the virial parameter is initially of order unity but decreases to  $\ll 1$  in a crossing time as turbulence decays (Bonnell *et al.*, 2004; Bate *et al.*, 2002a,b, 2003). It is also noteworthy that many of the simulations begin with clumps of mass consider-

ably smaller ( $M \leq 100M_{\odot}$ ) than that typically one found in star forming regions  $\sim 5000M_{\odot}$  (Plume *et al.*, 1997). Krumholz *et al.* (2005a) show that for competitive accretion to work,  $\alpha_{\text{vir}}^2 M < 10M_{\odot}$ , but for typical star forming regions  $\alpha_{\text{vir}} \approx 1$  and  $M \approx 10^2-10^4M_{\odot}$  and the inequality is almost never satisfied.

One reason why simulations evolve to  $\alpha_{\text{vir}} \ll 1$  is that they omit feedback from star formation. Observations by Quillen *et al.* (2005) show that outflows inject enough energy on the scale of a clump to sustain turbulence thereby keeping the virial parameter from declining to values much less than unity. Another possible reason is that the simulations consider isolated clumps with too little material. Real clumps are embedded in larger molecular clouds where larger scale turbulent motions can cascade down to the clump scale preventing the rapid decay of the turbulence.

### 5.3. 3D Collapse with Radiation

Radiation transfer is an important element in both low mass and high mass star formation. Boss *et al.* (2000) carried out the first 3D simulations including radiation transfer to study the effect of radiation on the formation of stars in collapsing molecular cloud cores. Starting from cores with Gaussian initial density profiles, this work compared collapse calculations based on the isothermal and barotropic approximations with the more realistic case of detailed radiative transfer in the Eddington approximation. The use of the isothermal equation of state resulted in a collapse leading to a thin isothermal filament (Truelove *et al.*, 1997). In the more realistic case with nonisothermal heating using radiative transfer in the Eddington approximation, they showed that thermal retardation of the collapse caused the formation of a binary protostar system at the same maximum density where the isothermal collapse yielded a thin filament. Eventually, the binary clumps evolved into a central protostar surrounded by spiral arms containing two more clumps. The corresponding collapse using the barotropic approximation allowed a transition from an isothermal optically thin to an optically thick flow. It resulted in a transient binary merging into a central object surrounded by spiral arms with no evidence of further fragmentation. The barotropic result differs significantly from the Eddington result at the same maximum density indicating the importance of detailed radiative transfer effects.

Boss *et al.* (2000) examined the differences in the use of a barotropic stiffened EOS approximation and radiative transfer. In the former, the thermal properties of the gas are specified solely as a function of density. This implies that a single global value of a critical density represents the entire calculation and its value depends weakly on the assumed geometry of the cloud (Inutsuka and Miyama, 1997). In 3-D the effective value of this critical density depends on the local geometry surrounding a fluid element. In addition, whereas the specific entropy of a gas parcel gener-

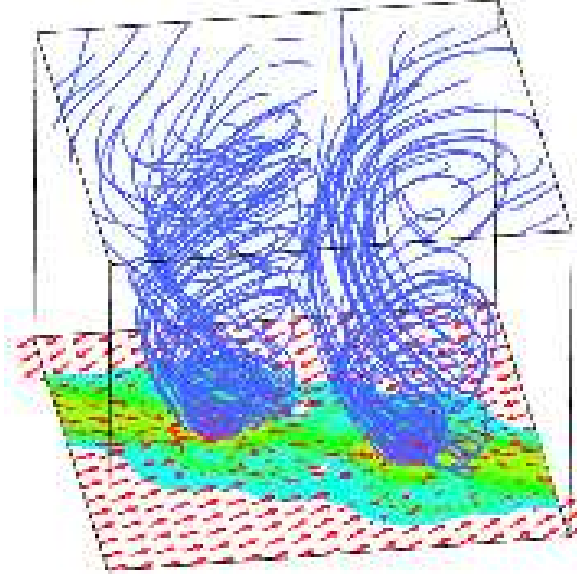


Fig. 1.— Binary outflows. Magnetic field lines, velocity field vectors and density distribution on the  $z = 0$  plane. Taken from model DL of *Machida et al* (2005b).

ally depends on the thermal history of the parcel, the specific entropy of the gas using the barotropic approximation depends solely on the density. Thus the derived pressures used in the momentum equations will differ between a calculation using a stiffened EOS approximation and a fully consistent calculation using radiative transfer. As a result, the temperature is determined not simply by adiabatic compression, but by compressional heating in a 3D volume with highly variable optical depth. Thus the dependence of the temperature on the density cannot be represented with a simple barotropic approximation with any great accuracy. This causes concern for the validity of current simulations of multiple star formation and cluster formation, since essentially all use either the isothermal or the barotropic approximation. Recent work by *Whitehouse and Bate* (2005) examined core collapse with radiation and the adequacy of the barotropic approximation as well.

#### 5.4. The Debate Over Disk Fragmentation

As pointed out in section 2, most simulations to date, performed with SPH, find circumstellar disk fragmentation and rapid ejection of BDs in most cases (*Bate et al.*, 2003; *Delgado-Donate et al.*, 2004; *Goodwin et al.*, 2004a,b) even possibly to an excess of BD and low-mass companions (*Goodwin et al.*, 2004b). Furthermore, most simulations are terminated at an arbitrary time, when much of the gas is still present; hence the simulations may provide only a lower bound to the number of companions that would be produced. As discussed in section 2, these simulations are increasingly contradicted by recent observations. *Goodwin and Kroupa* (2005) have recently pointed out that observations suggest that individual cores produce at most 2-3

protostars. A possible reason for this problem is the absence of a magnetic field and inaccurate thermodynamics (i.e. barotropic equation rather than radiative transfer) in the SPH simulations.

However, there is an alternative explanation: The SPH simulations are likely not converged. Indeed, recent high resolution AMR simulations of the collapse and fragmentation of turbulent cores (*Klein et al.*, 2004a,b) show that a magnetic field and radiative transfer is not required to explain the observational results of *Goodwin and Kroupa* (2005). *Klein et al.*, (2004a,b) find that over a broad range of turbulent Mach numbers ( $M \sim 1 - 3$ ) and rotational energies ( $\beta \sim 10^{-4} - 10^{-1}$ ) low order single or binary stars are formed through fragmentation of the core, not the ensuing disk. Is it then a matter of faith in one numerical method or the other? SPH versus AMR? Not really, it is rather a matter of testing the convergence of the numerical simulations, irrespective of the method.

*Fisher et al.* (2006, in preparation) have performed high resolution, full convergence studies using the SPH code Gadget with the same model and initial conditions as *Goodwin et al.* (2004a), except for the initial turbulent seed. They confirmed the results of *Goodwin et al.*, (2004a) at the same low resolution (only one smoothing kernel per minimum Jeans mass). But they have also found *no convergence* of either the multiple number of companion protostars produced or the time for multiple fragmentation to occur in the disk, with up to 32 times the resolution of *Goodwin et al.*, (2004a). This suggests that the current SPH simulations showing high order multiple disk fragmentation may be grossly under resolved. If so, the disagreement with the observations may not be due only to the absence of the magnetic field and radiation, but also to unconvolved numerics. Recent grid-based simulations attempting to study fragmentation in isolated disks (cf. *Durisen* this book) indicate that for 2D axisymmetric disk studies very high resolution, 256 cells in the radial direction alone (*Ostriker* private communication), is required to demonstrate that disks do not suffer from numerical instability. This level of resolution is far beyond any SPH simulation of cores or clusters to date showing disk fragmentation, and would be difficult to achieve also with AMR simulations starting from globally collapsing cores.

At the time of this conference, the debate between SPH and AMR with respect to the issue of disk fragmentation continues, but it is our strong opinion that all simulations using SPH or AMR must demonstrate adequate convergence to be credible. This should apply also to physical systems that may display chaotic behavior, such as the gas dynamics in a molecular cloud core. A high sensitivity to initial conditions may result in statistical distributions of the measured quantities (e.g., number of collapsing objects and their formation time) around some mean value. In this case, an expensive approach to test numerical convergence would consist of running a large number of experiments at each resolution and test for the convergence of the statistical distributions of the quantities of interest. A less expensive

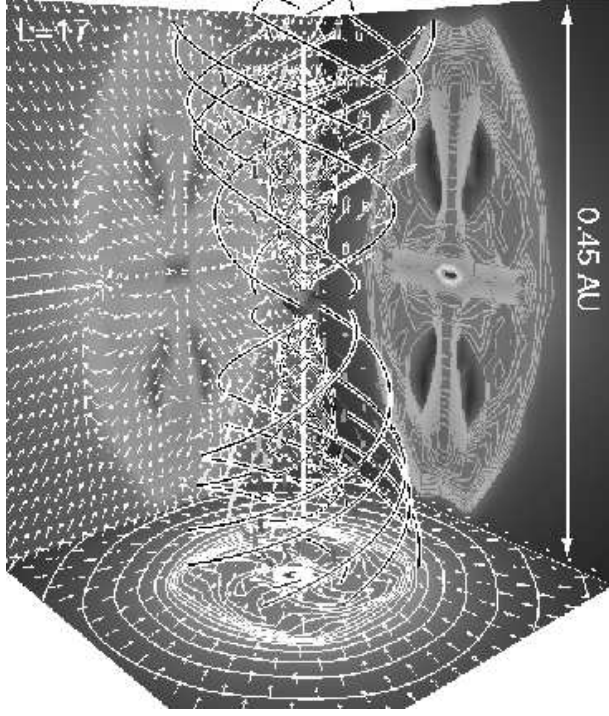


Fig. 2.— Bird's-eye view of the magnetic field lines in the fast jet emanating from the central region around a protostar. Only the 17th grid in the nested-grid resistive MHD calculations by *Machida et al.* (2006, in preparation) is shown. The density contours and velocity vectors are projected on the walls on both sides.

approach is to measure quantities with a weak sensitivity to initial conditions because they already represent the average of some statistical distribution, or just because they are even more sensitive to the numerical resolution than to the initial conditions. For example, *Fisher et al.* (2006) find that as they increase the resolution of their SPH simulations, the time of disk fragmentation (when the first object is formed) increases monotonically with resolution, a sign of lack of convergence in the SPH simulations, rather than a signature of chaotic behavior.

### 5.5. Star formation in a cloud with Magnetic Field and Rotation

**5.5.1. Fragmentation of the First Core.** A non-rotating cloud core without magnetic field contracts in a self-similar manner to form a first core that is composed of molecular hydrogen (*Larson*, 1969; *Masunaga et al.*, 1998). Recently, nested grid MHD simulations (*Machida et al.*, 2004, 2005a) have revealed that i) a rotating magnetized core evolves maintaining a ratio of angular speed to magnetic field strength at the center  $\Omega_c/B_c \simeq \text{const}$ ; and ii)  $\Omega_c$  and  $B_c$  are well correlated at the first core phase and satisfy the “magnetic flux – spin relation” as  $\Omega_c^2/0.2^2 4\pi G \rho_c + B_c^2/0.36^2 8\pi c_s^2 \rho_c \simeq 1$ , using a central density  $\rho_c$  and isothermal sound speed  $c_s$ . This is regarded as an appear-

ance of self-similarity in magnetized rotating cores.

The fragmentation of the first core is regarded as one of the mechanisms to explain close binary systems (*Bonnell and Bate*, 1994b; *Bate*, 1998). The magnetic field affects the rotational motion (magnetic braking) and thus the fragmentation. Whether the magnetic field stabilizes the first core against the fragmentation or not (*Machida et al.*, 2005b; *Ziegler*, 2005) is attracting attention in relation to the binary formation. As well as non-magnetic cores (see §3.a.5), a magnetized first core can fragment if it is rotating sufficiently fast,  $\Omega_c \simeq 0.2(4\pi G \rho_c)^{1/2}$  (*Machida et al.*, 2005b) and has only a weak magnetic field,  $B_c \lesssim 0.3(8\pi c_s^2 \rho_c)^{1/2}$ . Simulations show that increasing the magnetic field strength, fragmentation is stabilized by the suppression of rotational motion by magnetic braking (see also *Hosking and Whitworth*, 2004). This is not found by *Boss* (2002), but his model equation is not fully consistent with MHD and does not account for magnetic braking. In order to achieve enough rotation to cause fragmentation, the initial  $\Omega$ -to- $B$  ratio must satisfy the condition  $(\Omega/B)_{\text{init}} > 0.39 G^{1/2} c_s \sim 1.7 \times 10^{-7} (c_s/0.19 \text{ km s}^{-1})^{-1} \mu\text{G}^{-1}$  (*Machida et al.*, 2005b).

When  $\vec{B}$  and angular momentum  $\vec{J}$  are not parallel to each other, the magnetic braking works more efficiently for the component of  $\vec{J}$  perpendicular to  $\vec{B}$ . A magnetically dominated cloud core whose  $\Omega$ -to- $B$  ratio is less than the above critical value forms a disk perpendicular to the magnetic field (*Matsumoto and Tomisaka*, 2004) and an outflow is ejected in the direction of the local magnetic field, even if  $\vec{B}$  is not parallel to  $\vec{J}$ . The difference between the local field in the vicinity of a protostar and on the cloud scale is restricted to  $\lesssim 30$  deg for this case.

If the first core is fragmented into binary or multiple cores, each fragment spins and multiple outflows (Fig.1) are ejected (*Machida et al.*, 2004, 2005b; *Ziegler*, 2005; *Banerjee and Pudritz*, 2006), which explains binary outflows (*Liseau et al.*, 2005).

**5.5.2. Second Collapse with Magnetic Field.** Once the dissociation of molecular hydrogen starts at the central region of the first core, the second collapse begins. Further calculation of the evolution to form the second core (i.e., a protostar) requires the inclusion of resistivity in the MHD description, as the high density reduces the degree of ionization and the conductivity of the medium. *Machida et al.* (2006, in preparation) have adopted parametrized resistivity as a function of density in their nested-grid resistive MHD code, and extended the calculations of the collapse. During the isothermal phase, the magnetic Reynolds number is a decreasing function of density. If the magnetic Reynolds number decreases below unity, the magnetic field is effectively decoupled from the collapsing gas. However, the temperature of the gas becomes sufficiently high ( $\sim 10^3$  K) that the magnetic field is re-coupled again with the collapsing gas. This relatively sudden grab of the field lines tends to make a very collimated fast outflow around the second core. Fig. 2 shows a snapshot of the propagation of a fast

jet from the protostar. The density distribution on the cross section is also shown on the left and right walls. Note that bow shocks are clearly seen in the density plot. The results of this calculation indicate that a realistic modeling of the evolution of temperature and resistivity as a function of density is required for a precise description of the jet.

## 6. SUMMARY AND FUTURE DIRECTIONS

### 6.1. Summary

Observations of molecular clouds and cores provide a wealth of data that are important constraints for initial conditions of numerical simulations. Large scale simulations should be consistent with the turbulent nature of the ISM and the observed properties of prestellar cores should emerge self-consistently from the simulations. All calculations must adhere to the Jeans condition for grid-based schemes or a well established equivalent for particle-based schemes. It is important to stress that the Jeans condition is a necessary but not sufficient condition to guarantee avoidance of artificial fragmentation. Simulations must be tested at more resolved Jeans numbers to establish convergence.

The importance of turbulence in star formation is now well accepted. A very large spatial resolution is required to simulate the turbulent fragmentation, barely achieved by the largest grid-based simulations. Present SPH simulations fall several orders of magnitude below the required spatial resolution. It is possible that almost no available simulations have yet accurately tested the effect of turbulent fragmentation.

Magnetic fields play a crucial role in the star formation process. At this time there are no 3D, self-gravitational MHD simulations that have evolved stars from turbulent clouds. Grid based schemes such as AMR have developed high order accurate PPM and Godunov based MHD that can provide accurate solutions across several orders of magnitude of collapse. SPH has developed cruder approaches to MHD that appear to be rather poor even for very mild shocks, but this will hopefully improve. Godunov approaches to MHD for SPH may provide increased accuracy.

Radiation transport has been shown to play a significant role in the outcome of fragmentation to binary and multiple systems. It has been shown that side stepping the issue of radiation transport with a barotropic approximation can lead to incorrect results. Current AMR calculations have implemented radiation transfer in the flux-limited approximation and have used this for both low mass and high mass star formation. Radiation transfer schemes have recently been developed for SPH as well.

Current star formation simulations are not yet adequate to accurately span the many orders of magnitude of density and spatial range necessary to account for stars from initially turbulent clouds and encompassing all the relevant physics. In our opinion, AMR approaches with recent developments coupling radiation transfer and MHD hold out the best promise for achieving that goal. SPH, while making significant strides in the last few years, is still faced

with difficult challenges of accurate handling of turbulence, strong shocks, MHD, and radiation transfer. However, we anticipate further progress with SPH.

Current calculations are still not adequate to explain the stellar IMF. Of the two dominant theories for the origin of stellar masses described as direct gravitational collapse and competitive accretion, observations appear to favor the first. Recent theoretical work by *Krumholz et al.* (2005a) has now demonstrated that seed protostars cannot gain mass efficiently by competitive accretion processes in observed star-forming regions that are approximately in virial balance. There is no observational evidence for the existence of regions that are far from virial balance, as required by competitive accretion models. This suggests that competitive accretion is not a viable mechanism for producing the stellar IMF and that current simulations resulting in competitive accretion must have initial or boundary conditions inconsistent with the observations, or rather neglect some crucial physics. Theoretical efforts directed toward the picture of direct gravitational collapse set up by turbulent fragmentation appear to be more promising.

### 6.2. Future Directions for Numerical Simulation

The lack of demonstrated convergence for most simulations in the field presents us with uncalibrated results. We strongly emphasize that future simulations should demonstrate numerical convergence before detailed comparison with observations can be credible. Otherwise there is no way to normalize the accuracy of large scale simulations and the results of such simulations will not advance our understanding of low mass star formation. Convergence tests should be always carried out irrespective of the numerical approach. A better understanding of the numerical treatment of disk fragmentation must occur to clear up the current discrepancies between AMR and SPH.

Future simulations of low mass star formation must endeavor to include MHD and radiation transfer. With the development of accurate approaches to these processes, we can expect to see simulations become more relevant to addressing the observations. For simulations to make a real connection to the observations, detailed line profiles and continuum sub-mm and mm maps should be calculated with 3D radiative transfer codes. Approaches that go beyond the Eddington approximation and flux-limited diffusion such as  $S_N$  transport and Monte Carlo need further development to work efficiently in full 3D simulations. They will become increasingly important in treating the flow of radiation in highly inhomogeneous regions. As future simulations encompass multi-coupled physics, significant progress must be made in algorithms that improve the parallel scalability. That is necessary in order to simulate the full dynamic range of collapse and fragmentation from clouds to stars, while capturing all the relevant physics.

## REFERENCES

Allen A., Li Z.-Y., and Shu F. H. (2003) *Astrophys. J.*, 599, 363-379.

Alves J. F., Lada C. J., and Lada E. A. (2001) *Nature*, 409, 159-161.

Bacmann A., André P., Puget J.-L., Abergel A., Bontemps S., and Ward-Thompson D. (2000) *Astron. Astrophys.*, 361, 555-580.

Ballesteros-Paredes J., Gazol A., Kim J., Klessen R. S., Jappsen A.-K., and Tejero E. (2006) *Astrophys. J.*, 637, 384-391.

Ballesteros-Paredes J., Klessen R. S., and Vázquez-Semadeni E. (2003) *Astrophys. J.*, 592, 188-202.

Ballesteros-Paredes J. and Mac Low M.-M. (2002) *Astrophys. J.*, 570, 734-748.

Balsara D. S. and Kim J. (2004) *Astrophys. J.*, 602, 1079-1090.

Balsara D. S. and Spicer D. S. (1999) *J. Comp. Phys.*, 149, 270-292.

Banerjee R. and Pudritz R. E. (2006) *Astrophys. J.*, in press.

Banerjee R., Pudritz R. E., and Holmes L. (2004) *Mon. Not. R. Astron. Soc.*, 355, 248-272.

Barrado y Navascués D., Mohanty S., and Jayawardhana R. (2004) *Astrophys. J.*, 604, 284-296.

Bastien P., Cha S.-H., and Viau S. (2004) *Rev. Mex. Astron. Astrofis.*, 22, 144-147.

Basu S. and Mouschovias T. C. (1994) *Astrophys. J.*, 432, 720-741.

Bate M. R. (1998) *Astrophys. J.*, 508, L95-L98.

Bate M. R. and Bonnell I. A. (2005) *Mon. Not. R. Astron. Soc.*, 356, 1201-1221.

Bate M. R., Bonnell I. A., and Price N. M. (1995) *Mon. Not. R. Astron. Soc.*, 277, 362-376.

Bate M. R., Bonnell I. A., and Bromm V. (2002a) *Mon. Not. R. Astron. Soc.*, 332, L65-L68.

Bate M. R., Bonnell I. A., and Bromm V. (2002b) *Mon. Not. R. Astron. Soc.*, 336, 705-713.

Bate M. R., Bonnell I. A., and Bromm V. (2003) *Mon. Not. R. Astron. Soc.*, 339, 577-599.

Beresnyak A., Lazarian A., and Cho J. (2005) *Astrophys. J.*, 624, L93-L96.

Berger M. J. and Colella P. (1989) *J. Comp. Phys.*, 82, 64-84.

Blandford R. D. and Payne D. G. (1982) *Mon. Not. R. Astron. Soc.*, 199, 883-903.

Bodenheimer P., Burkert A., Klein R. I., and Boss A. P. (2000) In *Protostars and Planets IV* (V. Mannings et al., eds.), pp. 675-690. Univ. of Arizona, Tucson.

Boldyrev S. (2002) *Astrophys. J.*, 569, 841-845.

Boldyrev S., Nordlund Å., and Padoan P. (2002a) *Astrophys. J.*, 573, 678-684.

Boldyrev S., Nordlund Å., and Padoan P. (2002b) *Phys. Rev. L.*, 89, 031102-031105.

Bonnell I. A. (1994) *Mon. Not. R. Astron. Soc.*, 269, 837-848.

Bonnell I. A. and Bate M. R. (1994a) *Mon. Not. R. Astron. Soc.*, 269, L45-L48.

Bonnell I. A. and Bate M. R. (1994b) *Mon. Not. R. Astron. Soc.*, 271, 999-1004.

Bonnell I. A., Bate M. R., and Zinnecker H. (1998) *Mon. Not. R. Astron. Soc.*, 298, 93-102.

Bonnell I. A., Bate M. R., Clarke C. J., and Pringle J. E. (2001a) *Mon. Not. R. Astron. Soc.*, 323, 785-794.

Bonnell I. A., Clarke C. J., Bate M. R., and Pringle J. E. (2001b) *Mon. Not. R. Astron. Soc.*, 324, 573-579.

Bonnell I. A., Bate M. R., and Vine S. G. (2003) *Mon. Not. R. Astron. Soc.*, 343, 413-418.

Bonnell I. A., Vine S. G., and Bate M. R. (2004) *Mon. Not. R. Astron. Soc.*, 349, 735-741.

Bonnor W. B. (1956) *Mon. Not. R. Astron. Soc.*, 116, 351-359.

Bonnor W. B. (1957) *Mon. Not. R. Astron. Soc.*, 117, 104-117.

Boss A. P. (1981) *Astrophys. J.*, 250, 636-644.

Boss A. P. (2002) *Astrophys. J.*, 568, 743-753.

Boss A. P. and Myhill E. A. (1992) *Astrophys. J. Suppl.*, 83, 311-327.

Boss A. P., Fisher R. T., Klein R. I., and McKee C. F. (2000) *Astrophys. J.*, 528, 325-335.

Bourke T. L., Myers P. C., Robinson G., and Hyland A. R. (2001) *Astrophys. J.*, 554, 916-932.

Brio M. and Wu C. C. (1988) *J. Comp. Phys.*, 75, 400-422.

Burkert A., Bate M. R., and Bodenheimer P. (1997) *Mon. Not. R. Astron. Soc.*, 289, 497-504.

Byleveld S. E. and Pongracic H. (1996) *Publ. Astron. Soc. Pac.*, 13, 71-74.

Castor J. I. (2004) *Radiation Hydrodynamics*. Cambridge Univ. Press.

Cha S.-H. and Whitworth A. P. (2003a) *Mon. Not. R. Astron. Soc.*, 340, 73-90.

Cha S.-H. and Whitworth A. P. (2003b) *Mon. Not. R. Astron. Soc.*, 340, 91-104.

Chabrier G. (2003) *Publ. Astron. Soc. Pac.*, 115, 763-795.

Cho J., Lazarian A., and Vishniac E. T. (2003) *Astrophys. J.*, 595, 812-823.

Colella P. and Woodward P. R. (1984) *J. Comp. Phys.*, 54, 174-201.

Crockett R. K., Colella P., Fisher R. T., Klein R. I., and McKee C. F. (2005) *J. Comp. Phys.*, 203, 422-448.

Crutcher R. M. (1999) *Astrophys. J.*, 520, 706-713.

Crutcher R. M., Troland T. H., Goodman A. A., Heiles C., Kazes I., and Myers P. C. (1993) *Astrophys. J.*, 407, 175-184.

Crutcher R. M., Troland T. H., Lazareff B., Paubert G., and Kazès I. (1999) *Astrophys. J.*, 514, L121-L124.

Dai W. and Woodward P. R. (1994) *J. Comp. Phys.*, 115, 485-514.

Dedner A., Kemm F., Kröner D., Munz C.-D., Schnitzer T., and Wesenberg M. (2002) *J. Comp. Phys.*, 175, 645-673.

Delgado-Donate E. J., Clarke C. J., and Bate M. R. (2004) *Mon. Not. R. Astron. Soc.*, 347, 759-770.

Dimotakis P. E. (2000) *J. Fluid. Mech.*, 409, 69-98.

Dobler W., Haugen N. E., Yousef T. A., and Brandenburg A. (2003) *Phys. Rev. E*, 68, 026304-026311.

Dubrulle B. (1994) *Phys. Rev. L.*, 73, 959-962.

Duchêne G., Bouvier J., and Simon T. (1999) *Astron. Astrophys.*, 343, 831-840.

Duchêne G., Bouvier J., Bontemps S., André P., and Motte F. (2004) *Astron. Astrophys.*, 427, 651-665.

Dykema P. G., Klein R. I., and Castor J. I. (1996) *Astrophys. J.*, 457, 892-921.

Ebert R. (1957) *Zeitschrift Astrophys.*, 42, 263-272.

Edgar R. and Clarke C. (2004) *Mon. Not. R. Astron. Soc.*, 349, 678-686.

Elmegreen B. G. and Falgarone E. (1996) *Astrophys. J.*, 471, 816-821.

Esquivel A. and Lazarian A. (2005) *Astrophys. J.*, 631, 320-350.

Evans C. R. and Hawley J. F. (1988) *Astrophys. J.*, 332, 659-677.

Falgarone E., Puget J.-L., and Perault M. (1992) *Astron. Astrophys.*, 257, 715-730.

Falgarone E., Lis D. C., Phillips T. G., Pouquet A., Porter D. H., and Woodward P. R. (1994) *Astrophys. J.*, 436, 728-740.

Falkovich G. (1994) *Phys. Fluids*, 6, 1411-1414.

Fuller G. A. and Myers P. C. (1992) *Astrophys. J.*, 384, 523-527.

Galli D., Shu F. H., Laughlin G., and Lizano S. (2001) *Astrophys. J.*, **551**, 367-386.

Gammie C. F., Lin Y.-T., Stone J. M., and Ostriker E. C. (2003) *Astrophys. J.*, **592**, 203-216.

Goodman A. A., Benson P. J., Fuller G. A., and Myers P. C. (1993) *Astrophys. J.*, **406**, 528-547.

Goodwin S. P. and Kroupa P. (2005) *Astron. Astrophys.*, **439**, 565-569.

Goodwin S. P., Whitworth A. P., and Ward-Thompson D. (2004a) *Astron. Astrophys.*, **414**, 633-650.

Goodwin S. P., Whitworth A. P., and Ward-Thompson D. (2004b) *Astron. Astrophys.*, **423**, 169-182.

Gudiksen B. V. and Nordlund Å. (2005) *Astrophys. J.*, **618**, 1020-1030.

Haugen N. E. and Brandenburg A. (2004) *Phys. Rev. E*, **70**, 026405-026411.

Heiles C., Goodman A. A., McKee C. F., and Zweibel E. G. (1993) In *Protostars and Planets III* (E. H. Levy and J. I. Lunine, eds.), pp. 279-326. Univ. of Arizona, Tucson.

Heyer M. H. and Brunt C. M. (2004) *Astrophys. J.*, **615**, L45-L48.

Hosking J. G. and Whitworth A. P. (2004) *Mon. Not. R. Astron. Soc.*, **347**, 1001-1010.

Imamura J. N., Durisen R. H., and Pickett B. K. (2000) *Astrophys. J.*, **528**, 946-964.

Inutsuka S.-I. and Miyama S. M. (1997) *Astrophys. J.*, **480**, 681-693.

Jayawardhana R., Mohanty S., and Basri G. (2002) *Astrophys. J.*, **578**, L141-L144.

Jeans J. H. (1902) *Phil. Trans. A*, **199**, 1-53.

Jijina J., Myers P. C., and Adams F. C. (1999) *Astrophys. J. Suppl.*, **125**, 161-236.

Juvela M., Padoan P., and Nordlund Å. (2001) *Astrophys. J.*, **563**, 853-866.

Kitsionas S. and Whitworth A. P. (2002) *Mon. Not. R. Astron. Soc.*, **330**, 129-136.

Klein R. I. (1999) *Journ. Comp. and Applied Math.*, **109**, 123-152.

Klein R. I., Colella P., and McKee C. F. (1990) *Publ. Astron. Soc. Pac.*, **102**, 117-136.

Klein R. I., Fisher R. T., McKee C. F., and Truelove J. K. (1999) *numa.conf*, 131-140

Klein R. I., Fisher R., and McKee C. F. (2001) In *The Formation of Binary Stars* (H. Zinnecker and R. D. Mathieu, eds.), pp. 361-370.

Klein R. I., Fisher R. T., Krumholz M. R., and McKee C. F. (2003) *Rev. Mex. Astron. Astrofis.*, **15**, 92-96.

Klein R. I., Fisher R. T., McKee C. F., and Krumholz M. R. (2004a) *Publ. Astron. Soc. Pac.*, **323**, 227-234

Klein R. I., Fisher R., and McKee C. F. (2004b) *Rev. Mex. Astron. Astrofis.*, **22**, 3-7.

Klein R. I., Fisher R. T., McKee C. F., and Krumholz M. R. (2004c), In *Adaptive Mesh Refinement* (Tomasz Plewa, ed.), pp. 112-118. Chicago University Press

Klessen R. S. (2001) *Astrophys. J.*, **556**, 837-846.

Klessen R. S. and Burkert A. (2000) *Astrophys. J. Suppl.*, **128**, 287-319.

Klessen R. S. and Burkert A. (2001) *Astrophys. J.*, **549**, 386-401.

Klessen R. S., Ballesteros-Paredes J., Vázquez-Semadeni E., and Durán-Rojas C. (2005) *Astrophys. J.*, **620**, 786-794.

Koyama H. and Inutsuka S.-I. (2000) *Astrophys. J.*, **532**, 980-993.

Kritsuk A. G., Norman M. L., and Padoan P. (2006) *Astrophys. J.*, **638**, L25-L28.

Krumholz M. R., McKee C. F., and Klein R. I. (2004) *Astrophys. J.*, **611**, 399-412.

Krumholz M. R., McKee C. F., and Klein R. I. (2005a) *Nature*, **438**, 332-334.

Krumholz M. R., McKee C. F., and Klein R. I. (2005b) *Astrophys. J.*, **618**, 757-768.

Krumholz M. R., Klein R. I., and McKee C. F. (2005c) In *Massive star birth: A crossroads of Astrophysics* (R. Cesaroni et al., eds.), pp. 231-236. Cambridge University Press.

Krumholz M. R., McKee C. F., and Klein R. I. (2005d) *Astrophys. J.*, **618**, L33-L36.

Krumholz M. R., McKee C. F., and Klein R. I. (2006) *Astrophys. J.*, **638**, 369-381.

Lada C. J. and Lada E. A. (2003) *Ann. Rev. Astron. Astrophys.*, **41**, 57-115.

Larson R. B. (1969) *Mon. Not. R. Astron. Soc.*, **145**, 271-295.

Larson R. B. (1981) *Mon. Not. R. Astron. Soc.*, **194**, 809-826.

Li P. S., Norman M. L., Mac Low M.-M., and Heitsch F. (2004) *Astrophys. J.*, **605**, 800-818.

Liseau R., Fridlund C. V. M., and Larsson B. (2005) *Astrophys. J.*, **619**, 959-967.

Mac Low M.-M. and Klessen R. S. (2004) *Rev. Mod. Phys.*, **76**, 125-194.

Mac Low M.-M., Smith M. D., Klessen R. S., and Burkert A. (1998) *Astron. Astrophys. Suppl.*, **261**, 195-196.

Machida M. N., Tomisaka K., and Matsumoto T. (2004) *Mon. Not. R. Astron. Soc.*, **348**, L1-L5.

Machida M. N., Matsumoto T., Tomisaka K., and Hanawa T. (2005a) *Mon. Not. R. Astron. Soc.*, **362**, 369-381.

Machida M. N., Matsumoto T., Hanawa T., and Tomisaka K. (2005b) *Mon. Not. R. Astron. Soc.*, **362**, 382-402.

MacNeice P., Olson K. M., Mobarry C., de Fainchtein R., and Packer C. (2000) *Comp. Phys. Comm.*, **126**, 330-354.

Masunaga H. and Inutsuka S.-I. (1999) *Astrophys. J.*, **510**, 822-827.

Masunaga H. and Inutsuka S.-i. (2000a) *Astrophys. J.*, **531**, 350-365.

Masunaga H. and Inutsuka S.-i. (2000b) *Astrophys. J.*, **536**, 406-415.

Masunaga H., Miyama S. M., and Inutsuka S.-I. (1998) *Astrophys. J.*, **495**, 346-369.

Matsumoto T. and Hanawa T. (2003) *Astrophys. J.*, **595**, 913-934.

Matsumoto T. and Tomisaka K. (2004) *Astrophys. J.*, **616**, 266-282.

McKee C. F., Zweibel E. G., Goodman A. A., and Heiles C. (1993) In *Protostars and Planets III* (E. H. Levy and J. I. Lunine, eds.), pp. 327-342. Univ. of Arizona, Tucson.

McKee C. F. (1989) *Astrophys. J.*, **345**, 782-801.

McKee C. F. and Tan J. C. (2003) *Astrophys. J.*, **585**, 850-871.

Mihalas D. and Mihalas B. W. (1984) *Foundations of radiation hydrodynamics*. Oxford University, Oxford.

Mohanty S., Jayawardhana R., and Basri G. (2005) *Astrophys. J.*, **626**, 498-522.

Monaghan J. J. (1989) *J. Comp. Phys.*, **82**, 1-15.

Monaghan J. J. (1994) *J. Comp. Phys.*, **110**, 399-406.

Morris J. P. (1996) *Publ. Astron. Soc. Aus.*, **13**, 97-102.

Motte F., Andre P., and Neri R. (1998) *Astron. Astrophys.*, **336**, 150-172.

Motte F., André P., Ward-Thompson D., and Bontemps S. (2001) *Astron. Astrophys.*, **372**, L41-L44.

Mouschovias T. C. and Spitzer L. (1976) *Astrophys. J.*, **210**, 326-327.

Myers P. C., Dame T. M., Thaddeus P., Cohen R. S., Silverberg

R. F., Dwek E., and Hauser M. G. (1986) *Astrophys. J.*, **301**, 398-422.

Nakajima Y. and Hanawa T. (1996) *Astrophys. J.*, **467**, 321-333.

Nakano T., Nishi R., and Umebayashi T. (2002) *Astrophys. J.*, **573**, 199-214.

Natta A., Testi L., Muzerolle J., Randich S., Comerón F., and Persi P. (2004) *Astron. Astrophys.*, **424**, 603-612.

Nordlund Å. and Padoan P. (1999) In *Interstellar Turbulence* (J. Franco and A. Carraminana, eds.), pp. 218-231. Cambridge University Press.

Nordlund Å. and Padoan P. (2003) In *Turbulence and Magnetic Fields in Astrophysics* (E. Falgarone, and T. Passot, eds.), pp. 271-298. Springer.

Norman M. L. and Bryan G. L. (1999) In *Numerical Astrophysics* (S. M. Miyama et al., eds.), pp. 19-33. Kluwer Academic.

Nutter D. J., Ward-Thompson D., Crutcher R. M., and Kirk J. M. (2004) *Astron. Astrophys. Suppl.*, **292**, 179-184.

Ossenkopf V. (2002) *Astron. Astrophys.*, **391**, 295-315.

Ossenkopf V. and Mac Low M.-M. (2002) *Astron. Astrophys.*, **390**, 307-326.

Ostriker E. C., Gammie C. F., and Stone J. M. (1999) *Astrophys. J.*, **513**, 259-274.

Ostriker E. C., Stone J. M., and Gammie C. F. (2001) *Astrophys. J.*, **546**, 980-1005.

Padoan P. and Nordlund Å. (1997) astro-ph/9706177

Padoan P. and Nordlund Å. (1999) *Astrophys. J.*, **526**, 279-294.

Padoan P. and Nordlund Å. (2002) *Astrophys. J.*, **576**, 870-879.

Padoan P. and Nordlund Å. (2004) *Astrophys. J.*, **617**, 559-564.

Padoan P., Jones B. J. T., and Nordlund A. P. (1997) *Astrophys. J.*, **474**, 730-734.

Padoan P., Juvela M., Bally J., and Nordlund A. (1998) *Astrophys. J.*, **504**, 300-313.

Padoan P., Bally J., Billawala Y., Juvela M., and Nordlund Å. (1999) *Astrophys. J.*, **525**, 318-329.

Padoan P., Goodman A., Draine B. T., Juvela M., and Nordlund Å., Rögnvaldsson Ö. E. (2001a) *Astrophys. J.*, **559**, 1005-1018.

Padoan P., Juvela M., Goodman A. A., and Nordlund Å. (2001b) *Astrophys. J.*, **553**, 227-234.

Padoan P., Jimenez R., Juvela M., and Nordlund Å. (2004a) *Astrophys. J.*, **604**, L49-L52.

Padoan P., Jimenez R., Nordlund Å., and Boldyrev S. (2004b) *Phys. Rev. L.*, **92**, 191102-191105.

Padoan P., Krtsuk A., Norman M. L., and Nordlund Å. (2005) *Astrophys. J.*, **622**, L61-L64.

Passot T. and Vázquez-Semadeni E. (1998) *Phys. Rev. E*, **58**, 4501-4510.

Phillips G. J. and Monaghan J. J. (1985) *Mon. Not. R. Astron. Soc.*, **216**, 883-895.

Plume R., Jaffe D. T., Evans N. J., Martin-Pintado J., and Gomez-Gonzalez J. (1997) *Astrophys. J.*, **476**, 730-749.

Porter D. H. and Woodward P. R. (1994) *Astrophys. J. Suppl.*, **93**, 309-349.

Powell K. G., Roe P. L., Linde T. J., Gombosi T. I., and de Zeeuw D. L. (1999) *J. Comp. Phys.*, **154**, 284-309.

Price D. J. and Monaghan J. J. (2004a) *Mon. Not. R. Astron. Soc.*, **348**, 123-138.

Price D. J. and Monaghan J. J. (2004b) *Mon. Not. R. Astron. Soc.*, **348**, 139-152.

Price D. J. and Monaghan J. J. (2004c) *Astron. Astrophys. Suppl.*, **292**, 279-283.

Price D. J. and Monaghan J. J. (2005) *Mon. Not. R. Astron. Soc.*, **364**, 384-406.

Quillen A. C., Thorndike S. L., Cunningham A., Frank A., Gutermuth R. A., Blackman E. G., Pipher J. L., and Ridge N. (2005) *Astrophys. J.*, **632**, 941-955.

Reipurth B. and Clarke C. (2001) *Astron. J.*, **122**, 432-439.

Ryu D. and Jones T. W. (1995) *Astrophys. J.*, **442**, 228-258.

Ryu D. and Jones T. W., Frank A. (1995) *Astrophys. J.*, **452**, 785-796.

Ryu D., Miniati F., and Jones T. W., Frank A. (1998) *Astrophys. J.*, **509**, 244-255.

Scalo J., Vazquez-Semadeni E., Chappell D., and Passot T. (1998) *Astrophys. J.*, **504**, 835-853.

She Z.-S. and Leveque E. (1994) *Phys. Rev. L.*, **72**, 336-339.

Shu F. H., Adams F. C., and Lizano S. (1987) *Ann. Rev. Astron. Astrophys.*, **25**, 23-81.

Shu F. H., Laughlin G., Lizano S., and Galli D. (2000) *Astrophys. J.*, **535**, 190-210.

Snell R. L. et al. (2000) *Astrophys. J.*, **539**, L101-L105.

Stamatellos D. and Whitworth A. P. (2003) *Astron. Astrophys.*, **407**, 941-955.

Stamatellos D. and Whitworth A. P. (2005) *Astron. Astrophys.*, **439**, 153-158.

Stellingwerf R. F. and Peterkin R. E. (1994) *Mem. Soc. Astron. It.*, **65**, 991-1011.

Stone J. M. and Norman M. L. (1992a) *Astrophys. J. Suppl.*, **80**, 753-790.

Stone J. M. and Norman M. L. (1992b) *Astrophys. J. Suppl.*, **80**, 791-818.

Stone J. M., Ostriker E. C., and Gammie C. F. (1998) *Astrophys. J.*, **508**, L99-L102.

Sytine I. V., Porter D. H., Woodward P. R., Hodson S. W., and Winkler K.-H. (2000) *J. Comp. Phys.*, **158**, 225-238.

Tóth G. (2000) *J. Comp. Phys.*, **161**, 605-652.

Tilley D. A. and Pudritz R. E. (2004) *Mon. Not. R. Astron. Soc.*, **353**, 769-788.

Tomisaka K. (1998) *Astrophys. J.*, **502**, L163-167

Tomisaka K. (2000) *Astrophys. J.*, **528**, L41-L44.

Tomisaka K. (2002) *Astrophys. J.*, **575**, 306-326.

Tomisaka K., Ikeuchi S., and Nakamura T. (1988) *Astrophys. J.*, **335**, 239-262.

Tomisaka K., Ikeuchi S., and Nakamura T. (1989) *Astrophys. J.*, **341**, 220-237.

Troland T. H. and Heiles C. (1986) *Astrophys. J.*, **301**, 339-345.

Truelove J. K., Klein R. I., McKee C. F., Holliman J. H., Howell L. H., Greenough J. A., and Woods D. T. (1998) *Astrophys. J.*, **495**, 821-852.

Tsuribe T. and Inutsuka S.-I. (1999a) *Astrophys. J.*, **523**, L155-L158.

Tsuribe T. and Inutsuka S.-I. (1999b) *Astrophys. J.*, **526**, 307-313.

van Leer B. (1979) *J. Comp. Phys.*, **32**, 101-136.

Vazquez-Semadeni E. (1994) *Astrophys. J.*, **423**, 681-692.

Wada K. and Norman C. A. (2001) *Astrophys. J.*, **547**, 172-186.

Whitehouse S. C. and Bate M. R. (2004) *Mon. Not. R. Astron. Soc.*, **353**, 1078-1094.

Whitehouse S. C., Bate M. R., and Monaghan J. J. (2005) *Mon. Not. R. Astron. Soc.*, **364**, 1367-1377.

Wolfire M. G., Hollenbach D., McKee C. F., Tielens A. G. G. M., and Bakes E. L. O. (1995) *Astrophys. J.*, **443**, 152-168.

Yorke H. W., Bodenheimer P., and Laughlin G. (1993) *Astrophys. J.*, **411**, 274-284.

Yorke H. W. and Sonnhalter C. (2002) *Astrophys. J.*, **569**, 846-862.

Ziegler U. (2005) *Astron. Astrophys.*, **435**, 385-395.